Cell- and Region-Specific Expression of Depression-Related Protein p11 (S100a10) in the Brain

Ana Milosevic,[1]* Thomas Liebmann,[1] Margarete Knudsen,[1] Nicoletta Schintu,[2] Per Svenningsson,[2] and Paul Greengard[1]

[1]Laboratory of Molecular and Cellular Neuroscience, Rockefeller University, New York, New York, USA
[2]Section for Translational Neuropharmacology, Department of Clinical Neuroscience, CMM L8:01, Karolinska Institutet, 17176 Stockholm, Sweden

ABSTRACT

P11 (S100a10), a member of the S100 family of proteins, has widespread distribution in the vertebrate body, including in the brain, where it has a key role in membrane trafficking, vesicle secretion, and endocytosis. Recently, our laboratory has shown that a constitutive knockout of p11 (p11-KO) in mice results in a depressive-like phenotype. Furthermore, p11 has been implicated in major depressive disorder (MDD) and in the actions of antidepressants. Since depression affects multiple brain regions, and the role of p11 has only been determined in a few of these areas, a detailed analysis of p11 expression in the brain is warranted. Here we demonstrate that, although widespread in the brain, p11 expression is restricted to distinct regions, and specific neuronal and nonneuronal cell types. Furthermore, we provide comprehensive mapping of p11 expression using in situ hybridization, immunocytochemistry, and whole-tissue volume imaging. Overall, expression spans multiple brain regions, structures, and cell types, suggesting a complex role of p11 in depression. J. Comp. Neurol. 525:955–975, 2017.

INDEXING TERMS: p11; expression mapping; region-specificity; neurons; glia; endothelial cells; ependymal cells; meninges; depression; anti-GFP antibody RRID: AB_10073917; anti-GFP antibody RRID: AB_303395; anti-GFP antibody RRID: AB_300798; anti-GFP antibody RRID: AB_10000240; anti-p11 antibody RRID: AB_2183469; anti-NeuN antibody RRID: AB_2298772; anti-Aldh1L1 antibody RRID: AB_10712968; anti-GFAP antibody RRID: AB_305808; anti-Iba1 antibody RRID: AB_839504; anti-CNPase antibody RRID: AB_10122287; anti-Olig2 antibody RRID: AB_10861310; anti-NG2 antibody RRID: AB_177646

P11, also known as S100A10, calpactin I light chain, or annexin II light chain, is a protein that forms a heterotetramer complex with annexin A2 (Anxa2) (Gerke et al., 2005; Oh et al., 2013). This complex interacts with multiple types of receptors (Svenningsson et al., 2006; Warner-Schmidt et al., 2009), ion channels (Girard et al., 2002; Okuse et al., 2002; Donier et al., 2005), and enzymes (Le Bouffant et al., 1998; Mai et al., 2000; Zobiack et al., 2003). The p11/Anxa2 heterotetramer complex is involved in the organization of lipid microdomains on the cell membrane, bundling of actin filaments and cytoskeleton scaffolding, membrane trafficking, and fibrinolysis (Babiychuk and Draeger, 2000; Menke et al., 2005; Hayes et al., 2006; Surette et al., 2011). Although expressed in many organs, including the heart, kidneys, liver, lungs, spleen, testes, epidermis, aorta, thymus, gastrointestinal tract, and brain (Zimmer et al., 2005), little is known about the specificity of p11 expression within these organs. In addition to neurons, the expression of p11 has been confirmed in circulating monocytes/macrophages, endothelial cells in blood vessel walls, reactive astrocytes, splenocytes, fibroblasts, and tumor cells

Additional Supporting Information may be found in the online version of this article.

Grant sponsor: NIMH; Grant number: MH090963; Grant sponsor: NIDA; Grant number: DA010044; Grant sponsor: Leon Black Family Foundation; Grant sponsor: JPB Foundation; Grant sponsor: Fisher Center for Alzheimer's Research Foundation (to P.G.); Grant sponsor: Vetenskapsradet (to N.S. and P.S.). The content is solely the responsibility of the authors and does not necessarily represent the official views of the National Institutes of Health.

*CORRESPONDENCE TO: Ana Milosevic, Laboratory of Molecular and Cellular Neuroscience, Rockefeller University, New York, NY 10065. E-mail: amilosevic@rockefeller.edu

Received February 1, 2016; Revised August 3, 2016;
Accepted August 9, 2016.
DOI 10.1002/cne.24113
Published online October 21, 2016 in Wiley Online Library (wileyonlinelibrary.com)

(Gerke et al., 2005; Dassah et al., 2009; Madureira et al., 2012; Zamanian et al., 2012; Svenningsson et al., 2014).

The p11/Anxa2 system is involved in many diseases, such as thrombosis, atherosclerosis, retinopathy, pain perception, and cancer, as well as in neuropsychiatric diseases (Hedhli et al., 2012). Recently, the role of p11 in major depressive disorder (MDD) has garnered interest. A role for p11 in human neuropsychiatric disorders has been suggested in clinical studies (Anisman et al., 2008; Zhang et al., 2011a,b; Svenningsson et al., 2014). It was reported that patients with MDD and posttraumatic stress disorder have decreased levels of p11 in the brain (Svenningsson et al., 2006; Anisman et al., 2008; Alexander et al., 2010; Zhang et al., 2011b). Furthermore, p11 levels in white blood cells can predict a patient's response to antidepressants during the initial phase of treatment (Svenningsson et al., 2014). We have shown that the constitutive knockout of p11 in mice (p11-KO) results in a depressive-like phenotype (Svenningsson et al., 2006); this effect is replicated in region- and cell-specific knockouts (Alexander et al., 2010; Warner-Schmidt et al., 2012). Moreover, the p11 expressing cells in cortical layer 5a, and in mossy cells in the dentate gyrus, are critical for response to antidepressants, while those in the nucleus accumbens are not (Schmidt et al., 2012; Warner-Schmidt et al., 2012; Oh et al., 2013).

Taken together, these data point to a key role for p11 in MDD, but widespread expression in the brain makes it difficult to determine a unifying mechanism of p11 action. At present, it appears that p11-dependent changes in behavior vary in different regions and cell types, and are affected by the circuitry of each cell type. We and others have previously explored the role of p11 in MDD by examining individual neuronal subtypes, distinguished by position, neurotransmitter, and connectivity, and analyzing its mechanism of action in several areas, such as the cortex, nucleus accumbens, and hippocampus (Alexander et al., 2010; Schmidt et al., 2012; Warner-Schmidt et al., 2012; Oh et al., 2013; Lee et al., 2015). Other areas potentially important for the pathophysiology of depression such as the amygdala or midbrain monoaminergic nuclei, on the other hand, were not. To accomplish this, a detailed mapping of p11 expression is required. Here we provide the cell- and region-specific expression data of p11 in the adult mouse brain as revealed by in situ hybridization and immunofluorescence on tissue sections, as well as by immunolabeling enabled 3D imaging of solvent-cleared organs (iDISCO).

MATERIALS AND METHODS

Mouse lines

All methods using mouse lines were in accordance with the National Institutes of Health *Guide for the Care and Use of Laboratory Animals*. Protocols were approved by the Rockefeller University Institutional Animal Care and Use Committee (IACUC) and Karolinska Institutet standards.

P11-EGFP (S100a10-EGFP HC85; GENSAT (www.gensat.org) was obtained from the Mutant Mouse Regional Resource Center at the University of California at Davis, and was maintained in CD1 and C57BL/6 backgrounds. P11-TRAP mice (Schmidt et al., 2012), a gift from Dr. Heintz, were maintained on a C57BL/6 background. Wildtype (WT) and p11-KO mice were on C57BL/6 background (Svenningsson et al., 2006). Mice were housed on a 12-hour light/dark cycle and were provided water and food ad libitum at the Rockefeller University's animal facility. Adult mice (8 weeks to 8 months) of both sexes were selected for experiments.

Antibodies

Primary antibodies used in this study are listed in Table 1. All of the antibodies used for immunolabeling are commercially available from major companies. We used four different anti-GFP (green fluorescent protein) antibodies. The GFP antibody from Thermo Fisher (Waltham, MA; A-11122) has been generated using the GFP isolated from the jellyfish *A. victoria*, and validated in the corticotropin-releasing factor receptor CrhR1-GFP transgenic mouse line, detecting GFP in the CrhR1 cells (Justice et al., 2008). Two anti-GFP antibodies from Abcam (Cambridge, UK) were generated using the recombinant full-length GFP protein and validated by immunocytochemistry on the neurons from the reporter lines: ChIP grade polyclonal GFP antibody (Abcam, Cat. no. ab290) detected a reporter protein in the TH + cells isolated from the brain of the TH-EGFP (enhanced GFP) reporter mice (Fortin et al., 2012); rabbit polyclonal GFP (Cat. no. ab13970) has been validated on the serotoninergic varicosities in *Drosophila* strain UAS-mCD8-GFP (Chen and Condron, 2009). Chicken polyclonal anti-GFP antibody from Aves (Tigard, OR; GFP-1020), generated using purified recombinant GFP, was also validated in a reporter mouse line (Bang and Commons, 2012). The anti-p11 antibody was generated using the recombinant mouse p11 peptide (R&D Systems, Minneapolis, MN; Cat. no. AF2377). The antibody specificity has been validated on the brain tissue of the wildtype and p11-knockout mice; in the wildtype mice, antibody labeled layer5a cells, while no staining was observed on the brain tissue sections from the p11 knockout mouse (Schmidt et al., 2012). Anti-NeuN antibody (EMD Millipore, Bedford, MA; Cat. no. MAB377) was generated using the purified cell nuclei isolated from the mouse brain. The specificity of immunolabeling with this antibody was confirmed previously (Fricker-Gates et al.,

TABLE 1.
List of Antibodies

Antigen	Description of immunogen	Source, host species, cat. #, clone or lot #, RRID	Dilution used
GFP	GFP isolated from the jellyfish *Aequorea victoria*	Thermo Fisher Scientific, rabbit polyclonal, A-11122, RRID: AB_10073917	1/300-1/500
GFP	Recombinant full length protein corresponding to GFP	Abcam, rabbit polyclonal, ChIP grade, ab290, RRID: AB_303395	1/50
GFP	Recombinant full length protein corresponding to GFP	Abcam, chicken polyclonal, ab13970 RRID: AB_300798	1/300-1/500
GFP	Purified recombinant GFP	Aves, chicken polyclonal, GFP-1020, RRID: AB_10000240	1/2,000
P11 (S100a10)	*E. coli* derived recombinant mouse S100a10 Pro2-Lys97 Accession #PO8207	R&D Systems, goat polyclonal, AF2377 RRID: AB_2183469	1/200
NeuN	Purified cell nuclei from mouse brain	EMD Millipore, mouse monoclonal, MAB377, RRID: AB_2298772	1/500
Aldh1L1	Synthetic peptide conjugated to KHL derived from sequence 320-350 (ELA-TAEAVRSSWMRILPNVPEVEDSTDFFKS) of the mouse Adh1L1	Abcam, rabbit polyclonal, ab87117, RRID: AB_10712968	1/500
GFAP	Full length native protein (purified) corresponding to GFAP	Abcam, rabbit polyclonal, ab7260, RRID: AB_305808	1/500
Iba1	Synthetic peptide corresponding to C-terminus of Iba1, sequence N'-PTGPPAKKAISELP-C'	Wako, rabbit polyclonal, 019-19741, RRID: AB_839504	1/500
CNPase	46 kDa and 48 kDa subunits of the 94 kDa myelin CNPase dimer	Biolegend/Covance/Sternberger Monoclonals, mouse monoclonal, SMI-91, RRID: AB_10122287	1/500
Olig2	Synthetic peptide corresponding to a sequence 250-280 (SVGSIRPPHGLLKS-PSAAAAAPLGGGGGGSG) of the human Olig2	Abcam, rabbit polyclonal, ab109186, RRID: AB_10861310	1/500
NG2	Cell line expressing a truncated form of NG2	EMD Millipore mouse monoclonal, MAB5384, RRID: AB_177646	1/500

2004; Milosevic et al., 2008). Anti-aldh1l1 antibody (Abcam; Cat. no. ab87117). was generated using synthetic peptide of a mouse Aldh1l1, conjugated to the keyhole limepet hemocyanin. Antibody was previously confirmed to immunostain astrocytes (Tyzack et al., 2014). Anti-GFAP antibody (Abcam; Cat. no. ab7260) was generated using a full length of the native glial acidic fibrillary protein and it has been validated for detection of astrocytes (Liu et al., 2009). The immunostaining with both antibodies, Aldh1l1 and GFAP, matched staining of the astrocyte reporter lines, or astrocytes grown in vitro, that was done previously with the antibodies from different commercial sources (Raff et al., 1979; Milosevic and Goldman, 2002, 2004; Dougherty et al., 2012). Anti-Iba1 antibody (Wako, Osaka, Japan; Cat. no. 019-19741) was generated using the synthetic peptide corresponding to the C-terminus of the calcium-binding adaptor molecule 1. The antibody specifically labels ramified microglia in the central nervous system (CNS) (Benton et al., 2008). A monoclonal antibody to CNPase (BioLegend, San Diego, CA; Cat. no. SMI-91) was generated with the 46 kDa and 48 kDa subunits of the CNPase dimer. The antibody was extensively validated in the brain tissue, where it labels myelinating oligodendrocytes (Kim et al., 2003; Werner et al., 2007). Rabbit monoclonal Olig2 antibody (Abcam; Cat. no. ab109186) was generated using the synthetic peptide of the human Olig2. It was shown previously that the antibody labels oligodendrocyte lineage cells, including oligodendrogliomas (Doyle et al., 2008; Dougherty et al., 2012). Antibody to chondroitin sulfate proteoglycan NG2 (EMD Millipore; Cat. no. MAB5384) was purified from the cell line expressing a truncated form of NG2. The antibody labels oligodendrocyte progenitors and it was extensively validated in double- and triple-labeling studies with other cell specific markers (Gautier et al., 2015; Zonouzi et al., 2015). In this study, for each primary antibody used (Table 1), a control consisted of immunocytochemical labeling with the secondary antibody only, to assure that no unspecific labeling exists.

Tissue processing, immunocytochemistry, and imaging

Adult mice were deeply anesthetized with Nembutal and intracardially perfused with 2% (used for p11-EGFP)

or 4% (used for p11-TRAP) paraformaldehyde (PFA) solution and cryopreserved through a series of sucrose dilutions. A series of 20 μm cryostat sections were mounted on the glass slides and used for immunocytochemistry. Sections were air-dried, washed in phosphate-buffered saline (PBS) with 0.3% Triton-X 100 (PBST), and incubated in a solution of 2% normal goat serum or heat-inactivated normal donkey serum in PBS for 30 minutes to 1 hour, followed by overnight incubation with primary antibodies (listed in Table 1), followed by incubation in the appropriate Alexa Fluor secondary antibodies (Invitrogen, La Jolla, CA), all diluted in PBST. Sections were mounted with ProLong mounting solution containing a nuclear marker DAPI (Molecular Probes, Eugene, OR) and imaged on a confocal LSM710 (Zeiss, Thornwood, NY). Figures were produced from a series of Z-stack images using Fiji ImageJ (NIH, Bethesda, MD) software and presented either as a projection or a single optical section.

For anatomical analysis of expression sites, whole mouse brains were sectioned at 20 μm; every fifth section was mounted on a glass slide and labeled with the anti-GFP antibody in a single experiment. Slides were covered with ProLong containing DAPI, scanned on the Axio Scan Z1 (Zeiss), and analyzed with PanoramicView software (3DHistech). In addition, low-magnification images represent one 5 × 5-tiled image of a whole brain section, selected from a series of coronal sections, each 100 μm apart, throughout a whole brain. They were imaged on a confocal LSM710, which gives better resolution. From this series, representative images were prepared for presentation in Adobe Photoshop CS6 (San Jose, CA). Only brightness and contrast were adjusted for individual images as needed.

Brain regions were identified using the *Mouse Brain in Stereotaxic Coordinates* (Paxinos and Franklin, 2004) and the Allen Brain Atlas (http://mouse.brain.-map.org). We use the anatomical names of the brain structures as they appear in Paxinos and Franklin's mouse brain atlas.

In situ hybridization

The in situ hybridization probe against p11 was made by polymerase chain reaction (PCR) amplification of nucleotides 1–293 of the coding sequence of the mouse p11 gene. The PCR fragment was subcloned into the pCRII-TOPO vector (Invitrogen), which contains the promotor sites for T3 and T7 RNA polymerases. ^{35}S-labeled antisense and sense cRNA probes were prepared by in vitro transcription. The transcription was performed from 50–100 ng of linearized plasmid using [^{35}S]UTP (>1000 Ci/mmol; Du Pont NEN, Boston, MA) and T3 or T7 RNA polymerases, as described previously (Svenningsson et al., 2006). The probes were purified on a Sephadex G50 column and precipitated in sodium acetate (0.1 vol) / absolute ethanol (2.5 vol).

Cryostat sections (14 μm) from wildtype, p11-EGFP, or p11-KO mice were postfixed in 4% PFA for 5 minutes at room temperature, rinsed twice in 4× sodium chloride–sodium citrate buffer (SSC), and placed into 0.25% acetic anhydride in 0.1 M triethanolamine / 4× SSC (pH 8) for 10 minutes at room temperature. After dehydration in graded alcohols, the sections were hybridized overnight at 55°C with 10^6 c.p.m. of ^{35}S-labeled p11 probe in 50 μl of hybridization solution (20 mM Tris–HCl / 1 mM EDTA / 300 mM NaCl / 50% formamide / 10% dextran sulphate / 1× Denhardt's / 250 μg/ml yeast tRNA / 100 μg/ml salmon sperm DNA / 0.1% SDS / 0.1% sodium thiosulphate). The slides were washed in 4× SSC (5 minutes, four times), RNAse A (20 μg/ml) (20 minutes, at 37°C), 2×SSC (5 minutes, twice), 1× SSC (5 minutes), 0.5×SSC (5 minutes) at room temperature, and rinsed in 0.1× SSC at 65°C (30 minutes, twice) (all washes contained 1 mM DTT), before being dehydrated in graded alcohols.

Sections were exposed on Kodak MR films for 4 weeks. Autoradiograms were scanned and digitized (Epson) and p11 mRNA expression was determined throughout the rostrocaudal axis according to the *Mouse Brain in Stereotaxic Coordinates* (Paxinos and Franklin, 2004).

iDISCO volume imaging

Tissue permeabilization

Brain hemispheres were treated according to the iDISCO protocol (Renier et al., 2014). Briefly, PFA-fixed brains were gradually dehydrated with methanol in PBS (50% ×1, 80% ×1, 100% ×2). The tissue was then bleached with a 1:5 ratio of hydrogen peroxide:methanol at 4°C. Samples were then rehydrated by removing methanol in 20% increments, followed by two washes in PBS. Finally, the samples were washed twice in PBS with 0.2% Triton X-100. Each wash step was 1 hour at room temperature.

iDISCO labeling

Hemispheres were treated overnight with PBS containing 0.2% Triton X-100 and 0.3 M glycine at 37°C, followed by blocking in PBS with 0.2% Triton X-100 and 6% normal goat serum. After blocking, samples were washed twice in PBS with 0.2% Tween-20 and 10 μg/ml heparin. Antibody labeling and subsequent washing steps were performed in the same solution. GFP was immunolabeled with anti-GFP antibodies and revealed by goat antirabbit secondary antibodies and To-Pro-3 nuclear stain (Life Technologies, Bethesda, MD), each with addition of 3% normal goat serum. Excess primary and secondary antibodies were washed for 24 hours

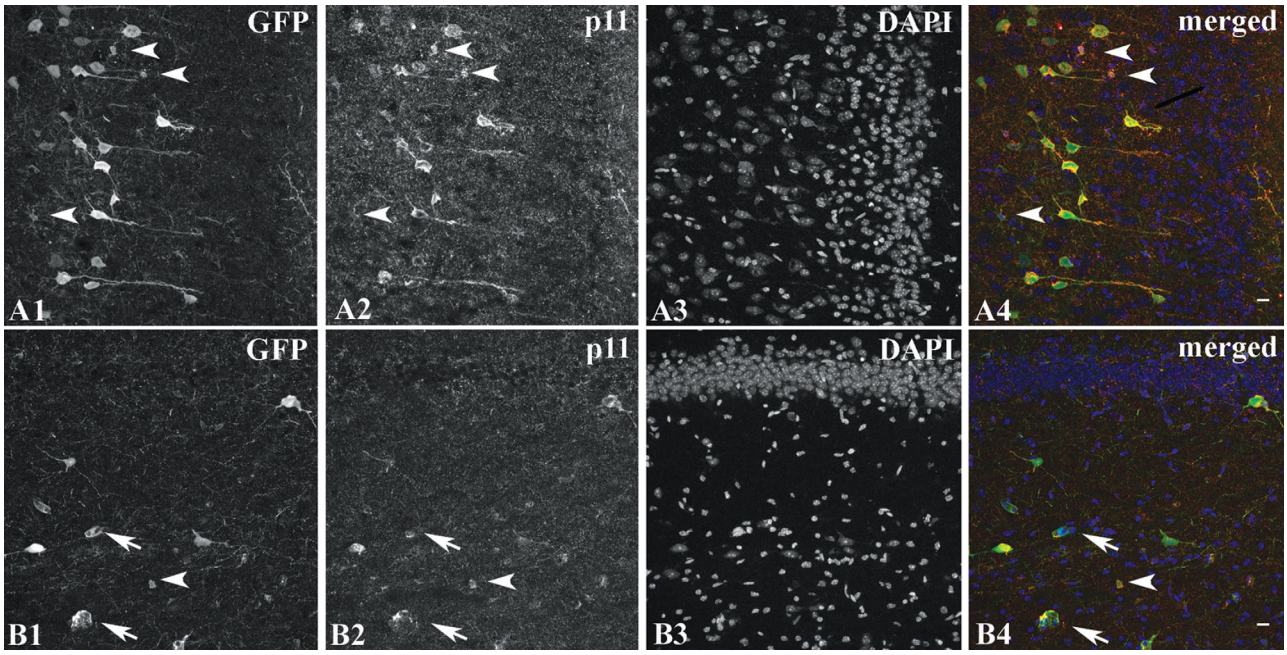

Figure 1. Native p11 protein colocalizes with the expression of GFP in the p11-EGFP transgenic mouse line. **(A1–4)** Pyramidal cells in the cingulate cortex of p11-EGFP mouse labeled with anti-GFP antibody (green), and anti-p11 antibody (red). **(B1–4)** Scattered double-labeled interneurons can be observed in the hippocampus. In both A and B, colabeling is also observed in glial cells (arrowhead) and blood vessels (arrows). Scale bars = 20 μ.

and 48 hours, respectively. Blocking and following staining incubation times were 5 days each.

Tissue clearing and imaging

Labeled samples were cleared according to the published iDISCO protocol (Renier et al., 2014). Tissue was dehydrated with tetrahydrofuran in water (50% ×1, 80% ×1, 100% ×2), then lipids were extracted in dichloromethane. Each step was performed for 1 hour at room temperature with gentle shaking. Finally, samples were rendered transparent with dibenzyl ether. Dehydration and lipid clearing steps were performed with 10 ml volumes in solvent-resistant scintillation vials. The vial was filled with dibenzyl ether to prevent sample oxidation. Imaging was performed on a light-sheet ultramicroscope (Ultramicroscope II, LaVision Biotec, Bielefeld, Germany) provided by the Bio-Imaging Resource Center at Rockefeller University. The samples were submerged in dibenzyl ether during imaging. Images were acquired with 16-bit depth with an axial plane spacing of 2.5 μm. Videos were generated with Imaris visualization software (Bitplane) using gamma correction to reveal the broad range of intensity values.

Single cell intensity measurements

Intensity measurements were made from whole hemispheres stained and cleared with iDISCO. Staining for intensity quantification was performed with anti-GFP (Aves, GFP-1020) antibody at 5 μg/ml. All other staining was done with the anti-GFP antibody (Abcam, ab290). Images were acquired on a light sheet microscope with a high-magnification objective (4× magnification plus a 2× optovar), and cells in seven representative areas were detected using SpotDetection from the ClearMap volume image analysis software package (Renier et al., 2016). Detection parameters were set according to the cell size and background intensity for each region. Values presented are maximum intensity after background subtraction.

RESULTS

GFP immunoreactivity represents p11 expression accurately in p11-EGFP mouse line

Analysis of the distribution of p11 in the brain, and specifically in morphologically distinct cell types, is challenging because of the low mRNA levels (Zimmer et al., 2005). Transgenic mouse lines, generated using Bacterial Artificial Chromosomes (BAC) that express EGFP under the control of all the regulatory regions of a given gene, offer analysis of the distinct cell types using immunostaining with anti-GFP antibody (Gong et al., 2003). For this study, we took advantage of a line that expresses EGFP (p11-EGFP HC85, www.

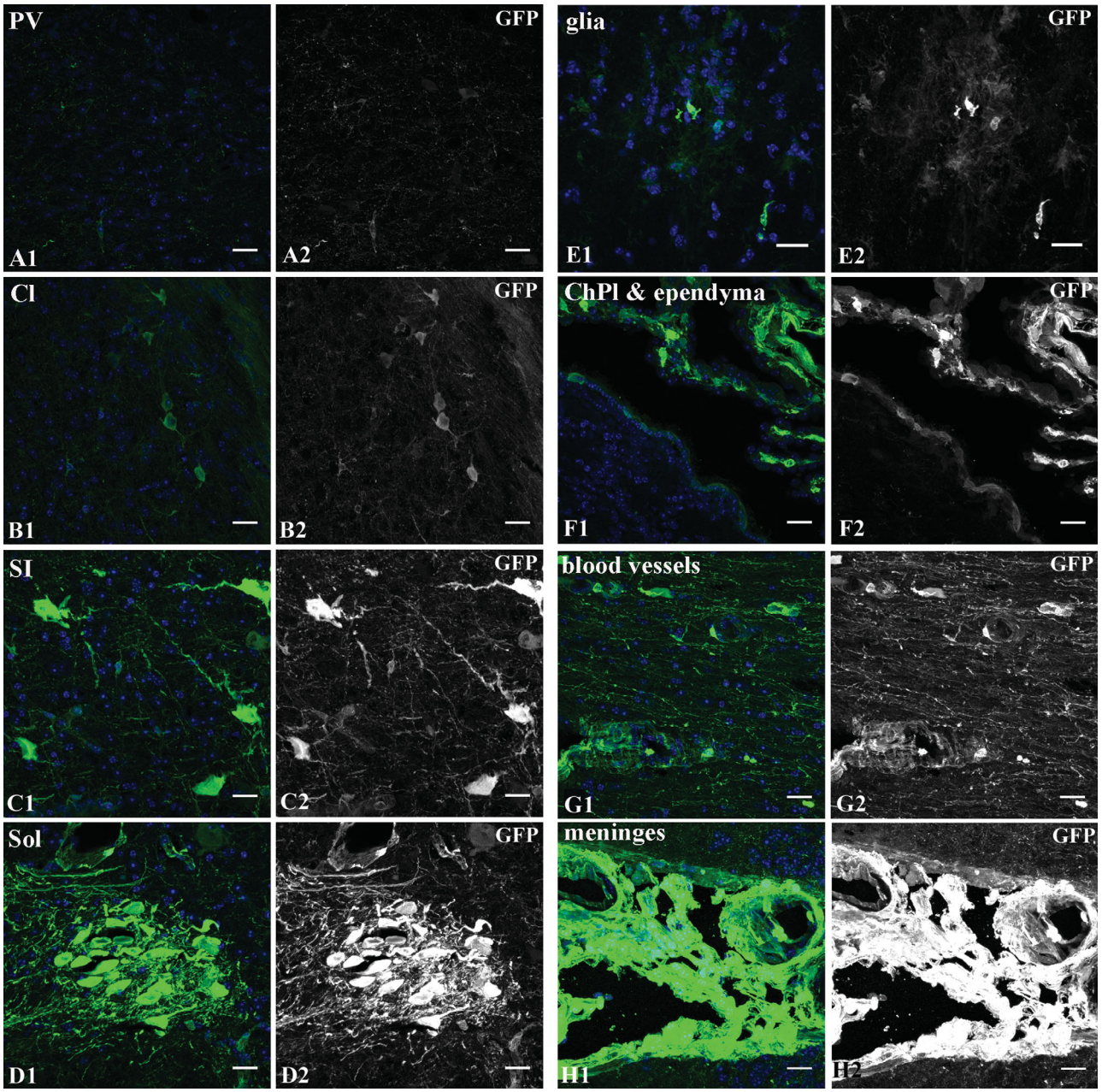

Figure 2. Multiple cell types express p11 throughout the brain. The GFP immunoreactivity in neurons is shown in A–D, and nonneuronal expression is shown in E–H. A1–H1 images depict brain areas with GFP + cells counterstained with DAPI to show the structure delineations, while A2–H2 images show only GFP immunoreactivity. Neuronal expression: **(A1–2)** Neurons in the paraventricular nucleus of the thalamus (PV), **(B1–2)** claustrum (Cl), a subregion of the cortex, **(C1–2)** substantia innominata (SI), a nucleus in the basal forebrain, and **(D1–2)** neurons in the solitary nucleus (Sol). Nonneuronal expression: GFP immunoreactivity is found in **(E1–2)** glial cells, **(F1–2)** ependymal cells (arrowheads), and subset of choroid plexus cells (arrows), **(G1–2)** cells comprising the blood vessel walls, and **(H1–2)** meninges. Scale bars = 20 μ.

gensat.org) and one that expresses EGFP fused with the ribosomal subunit L10a (p11-TRAP; Schmidt et al., 2012), both driven by p11 promoter activity. The high quality of immunostaining is enabled by the high copy numbers of the BAC in these lines, and exceeds the quality of immunocytochemical analysis using p11 antibodies.

First, we wanted to confirm that GFP expression localizes to the same cells as the native p11 protein in the p11-EGFP line. Brain sections were immunolabeled with the commercially available anti-p11 and anti-GFP antibodies (Table 1). The mouse anti-p11 antibody colocalized with the GFP immunoreactivity in the p11-EGFP line, and the representative image depicting the

TABLE 2.

List of Brain Regions and Corresponding Subregions Containing GFP + Neurons and In Situ Hybridization Signal

REGION	SUBREGION
OLFACTORY BULB	Gl-glomerular cell layer
	GrO-granule cell layer
	Mi-mitral cell layer
CORTEX	FrA, LO, AI, S, Cg, Au, V, Ect, PRh, Ent, RS, PrL, IL, Pir, M1, M2
AMYGDALA	CxA-cortex-amygdala transition zone
	BLA-basolateral amygdaloid nucleus
	BMA-basomedial amygdaliod nucleus
	MePD-medial amygdaloid nucl. posterodorsal
	MePV-medial amygdaloid nucl. posteroventral
	PMCo-posteromedial cortical amygdaloid area
	EA-extended amygdala
HIPPOCAMPUS	DG-dentate gyrus
	CA3 in ventral Hippocampus
	Sub-subiculum
STRIATUM	CPU-caudate putamen
	NAC-nucleus accumbens
	GP-globus pallidus
SEPTUM	LS-lateral septal nucleus, dorsal and ventral
	MS-medial septal nucleus
BASAL FOREBRAIN	VDB-ventral limb of the diagonal band nucl
	SI-substantia inominata
	VP-ventral pallidum
	HDB-horizontal limb of the diagonal band nucl
	MCPO-magnocellular nucleus
	BNST-bed nucleus of the stria terminalis
THALAMUS	AD-anterodorsal thalamic nucleus
	PV-paraventricular thalamic nucleus
	Hb-habenula
	VPL-ventral posterolateral thalamic nucleus
	VPM-ventral posteromedial thalamic nucleus
	OPC-oval paracentral nucl
	DLG-dorsal lateral geniculate nucleus
HYPOTHALAMUS	LH-lateral hypothalamus
	LPO-lateral preoptic area
	Pa-paravetricular hypothalamic nucleus
	DM-dorsomedial hypothalamic nucleus
	PH-posterior hypothalamic nucleus
MIDBRAIN	SN-VTA-substantia nigra, ventral tegmental area
	SC-superior colliculus, superficial gray layer
	SubB-subrachial nucleus
	RN-red nucleus
	PAG-periaqueductal gray
	DR-Dorsal raphe
	Me5-mesencephalic trigeminal nucleus
	3N-occulomotor nucleus
	IP-interpeduncular nucleus
	PBG-parabigeminal nucleus
	mRt-midbrain reticular nucleus
	LDTg-laterodorsal tegmental nucleus
CEREBELLUM	PC-Purkinje cell layer
PONS & MEDULLA	MnR-median raphe nucleus
	DRc-dorsal raphe caudal part
	DRi-dorsal raphe, interfascicular
	PTg-pedunculopontine tegmental nucleus
	PnO-pontine tegmental nucleus
	RtTg-reticular tegmental nucleus of pons
	LC-locus coeruleus
	Amb-ambiguous nucleus
	DTg-dorsal tegmental nucleus
	MBP-medial parabrachial nucleus
	DC-cochlear nucleus
	PnC-pontine reticular nucleus
	Gi-gigantocellular reticular nucleus
	DPGi-dorsal paragigantocellular nucleus
	RMg-raphe magnus nucleus
	Ve-vestibular nucleus
	IO-inferior olivary nucleus
	Sol-solitary nucleus
	Pr-prepositus nucleus
	Cu-cuneate nucleus
	Sp5-spinal trigeminal nucleus
	AP-area postrema
	Gr-gracile nucleus
	5N-motor trigeminal nucleus
	6N-abducens nucleus
	7N-facial nucleus
	10N-dorsal motor nucleus of the vagus
	12N-hypoglossal nucleus
	acs7-accessory facial nerve
	sp5-spinal trigeminal tract

The anatomical structures were delineated using the Paxinos and Franklin's Mouse Brain Atlas (Paxinos and Franklin, 2004) and Allen Brain Atlas (mouse.brain-map.org) and abbreviations are as shown in Paxinos and Franklin's Mouse Brain Atlas. Abbreviations for cortical areas: FrA-frontal association cortex, LO-lateral orbital cortex, AI-agranular insular cortex, S-somatosensory cortex, Cg-cingulate cortex, RS-retrosplenial cortex, Au-auditory cortex, V-visual cortex, Ect-ectorhinal cortex, PRh-perirhinal cortex, Ent-entorhinal cortex, Pir-piriform cortex, PrL-prelimbic cortex, IL-infralimbic cortex, M1 and M2-primary and secondary motor cortex.

cingulate cortex and hippocampus immunolabeled with the anti-GFP and anti-p11 antibodies is shown in Figure 1. In addition, we compared two mouse strains, C57BL/6 and CD1, and we did not detect differences in the immunofluorescent GFP signal (data not shown). Next, we confirmed that the p11-EGFP and p11-TRAP lines have comparable patterns of expression. GFP immunoreactivity was detected in neurons, cells in blood vessel walls, ependymal cells, and meninges (data not shown). However, glial cells were labeled with GFP antibody only in the p11-EGFP line. P11 transcripts

have been detected in astrocytes (J.P. Roussarie and A. Milosevic, pers. commun., and Zamanian et al., 2012), which suggests that the p11-EGFP line more accurately represents the p11 expression pattern in the brain than the p11-TRAP line. Thus, we decided to use this line in further analysis. All together, these data confirmed that p11-EGFP transgenic mouse line could be used to verify the expression pattern and cell types expressing p11 based on the GFP immunocytochemistry.

P11 is differentially expressed in multiple brain regions

We implemented immunocytochemistry using an anti-GFP antibody on tissue from the p11-EGFP transgenic mouse to comprehensively map the brain regions containing GFP-immunolabeled (GFP+) cells. GFP + cells were observed throughout the brain. Broadly, they can be classified as neuronal and nonneuronal, as shown in Figure 2. Neuronal expression is in some but not all brain regions (Table 2, Figs. 2–8, Supplemental Movies S1–3), while nonneuronal expression appears to be widespread (Figs. 2 and 9, Movies S1–3). Although all major brain regions contain GFP + neurons, their distribution is localized in discrete nuclei and often limited to a subpopulation of neurons within each structure. For example, only a subpopulation of neurons within the dorsal raphe nuclei are double-labeled with the antibodies to GFP and the neuronal marker NeuN (Fig. 4A1–4). Furthermore, GFP expression in the cortex is predominantly confined to layer 5a; only scattered GFP + neurons can be found in the upper and deep layers (Fig. 8A1–2). Similarly, in the hippocampus only a subset of neurons, namely, scattered interneurons in the molecular layer, and basket and mossy cells in the dentate gyrus, are GFP + (Fig. 8B1–3). By contrast, in some areas such as the motor trigeminal nucleus (5N) all NeuN + neurons also express GFP (Fig. 4B1–4). Nonneuronal GFP + cells are widespread in the brain, and they include glia (Fig. 2E1–2), choroid plexus, and ependymal cells (Fig. 2F1–2), endothelial (Fig. 2G1–2), and meningeal (Fig. 2H1–2) cells.

Neurons also display different intensities of the GFP immunolabeling (Fig. 3). The intensity was measured in seven representative brain regions with neuronal expression: ambiguous nucleus (Fig. 3A), basal forebrain, basomedial amygdala (Fig. 3B), dorsal raphe (Fig. 3C), locus coeruleus (Fig. 3D), medial amygdaloid nucleus (Fig. 3E), and ventral tegmental area (Fig. 3F). A graph showing the median single cell intensity is shown in Fig. 3G.

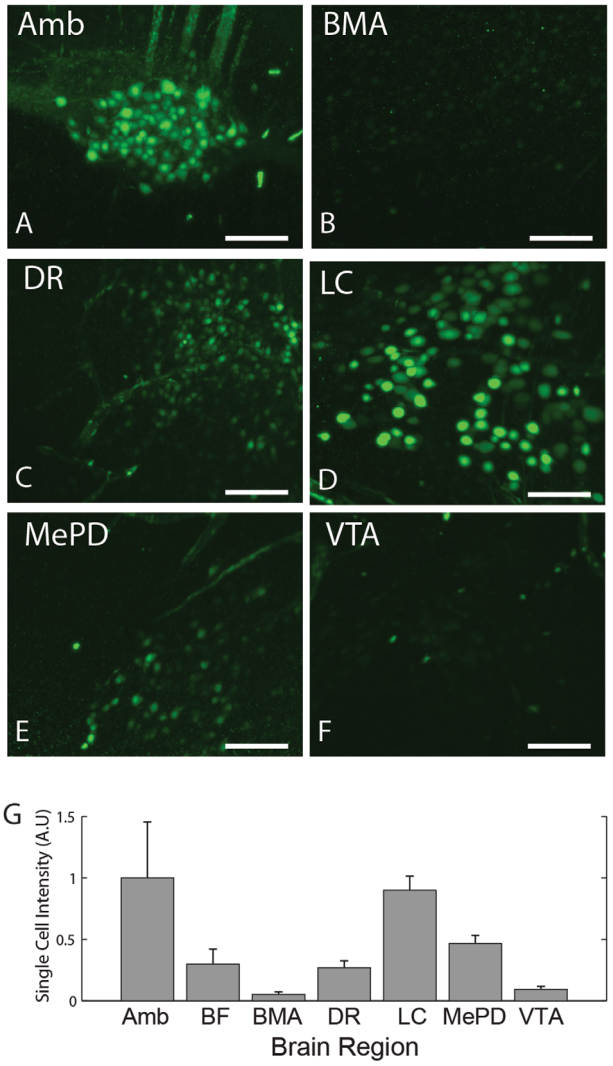

Figure 3. Neurons express different levels of p11 throughout the brain. **(A–F)** Representative maximum projections of light sheet microscope image stacks from the indicated region of intact p11-EGFP adult mouse brain. Brightness is enhanced in images for improved visibility of low level expression. **(G)** Mean values of single cell maximum GFP expression intensity detected in sample regions after local background subtraction. Relative single cell intensities are normalized by the brightest group (Amb). Error bars = represent standard deviation of the mean values from the three imaged intact brains. Amb, ambiguous nucleus; BF, basal forebrain; BMA, basomedial amygdaloid nucleus; DR, dorsal raphe; LC, locus coeruleus; MePD, medial posterior amygdaloid nucleus; VTA, ventral tegmental area. Scale bars = 100 μm.

Mapping of p11 expression in the brain

We sought to generate a detailed expression map of p11 protein and mRNA in the adult mouse brain. The analysis was done on a series of coronal sections, either immunolabeled with the GFP antibody, or detected using p11-specific RNA probe. The fluorescent and hybridization signals were found throughout the

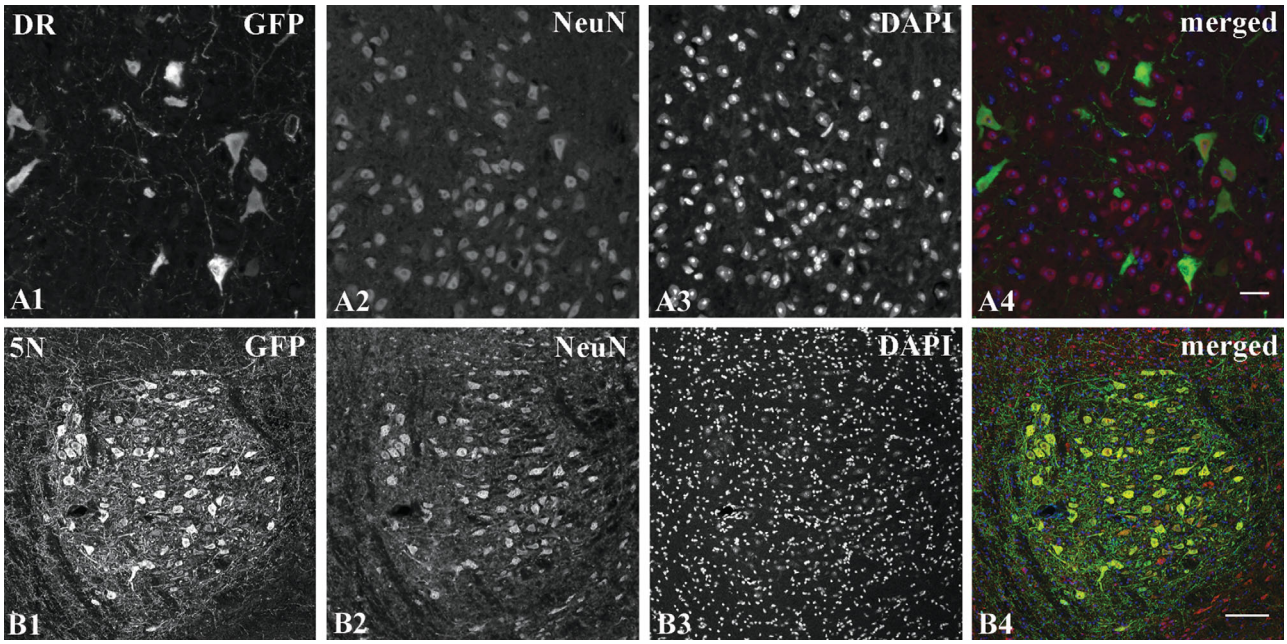

Figure 4. P11 is differentially expressed in neurons within structures in the brain. **(A1–4)** The upper row shows that in the dorsal raphe (DR) only a subset of GFP + neurons (green) are labeled with the neuronal marker NeuN (red), while lower row in **(B1–4)** motor trigeminal nucleus (5N) contains neurons labeled with both anti-GFP (green) and anti-NeuN (red) antibody, showing that all 5N neurons express p11. Scale bars = 20 μ in A; 100 μ in B.

entire mouse brain, but within distinct brain regions (Fig. 5 and Table 2). A detailed list of structures is summarized in Table 2.

Cortex contains a large number of GFP + pyramidal neurons, mainly in layer 5a (Fig. 5A–O, and a small number of neurons in layers 2 and 3, and deep layers 6a and 6b (Fig. 8A1). In the dorsolateral entorhinal cortex, strong expression is observed in layer 4/5 (Fig. 8A2).

Along with the mossy and basket cells in the dentate gyrus (Fig. 8B2), the hippocampus contains a small number of strongly stained GFP + cells scattered in the molecular layer (Fig. 8B1, Movie S3), and GFP + pyramidal neurons in the subiculum of the ventral hippocampus (Fig. 8B3). Low immunoreactivity was also observed in ventral hippocampal CA3 pyramidal neurons (data not shown).

GFP staining is restricted to a small number of scattered neurons in both dorsal and ventral striata (Fig. 5 and Movie S1). Expression in the basal forebrain, the main output of forebrain cholinergic innervation, is restricted to several nuclei (Table 2) with scattered GFP + cells (Figs. 2–8C1–2).

The amygdala, has GFP + cells in numerous nuclei (Table 2, Figs. 5, 8D1-2, Movies S1, S2). The basolateral amygdaloid nucleus, shown in Figure 8D1, contains a large number of GFP + cells, while central (Fig. 8D1), basomedial, and cortical amygdalar areas display signal in a subset of neurons (Fig. 8D2).

The thalamus has relatively low GFP expression overall, evident on the whole-tissue level (Fig. 5, Movie S1). The anterodorsal and ventromedial thalamic nuclei have small subpopulations of GFP + cells with high immunoreactivity (Table 2). In contrast, the hypothalamus contains many nuclei with strong GFP staining (Table 2). For example, the hypothalamic paraventricular nucleus (Fig. 8E, Movies S1, S2), and the lateral hypothalamus (Fig. 5) contain GFP + cells.

The midbrain contains a small number of nuclei with very strong GFP staining (Figs. 8F1–3, 8G). The dorsal raphe nuclei that provide major serotonergic innervation have a large number of GFP + cells (Fig. 8F1–3, Movie S2). Some nuclei with dopaminergic neurons, such as the substantia nigra, ventral tegmental area, and parabrachial pigmented area, have low GFP expression (Table 2, Fig. 3F). In contrast, the retrorubral field, also known as the A8 dopaminergic midbrain nucleus, has very strong GFP staining. Additionally, the red nucleus and mesencephalic trigeminal nucleus have cells with high GFP expression (Fig. 7H,I). The pons and medulla are the brain regions with the highest GFP immunoreactivity (Figs. 3, 5, Movies S1, S2). This includes the locus coeruleus, the main output for noradrenergic

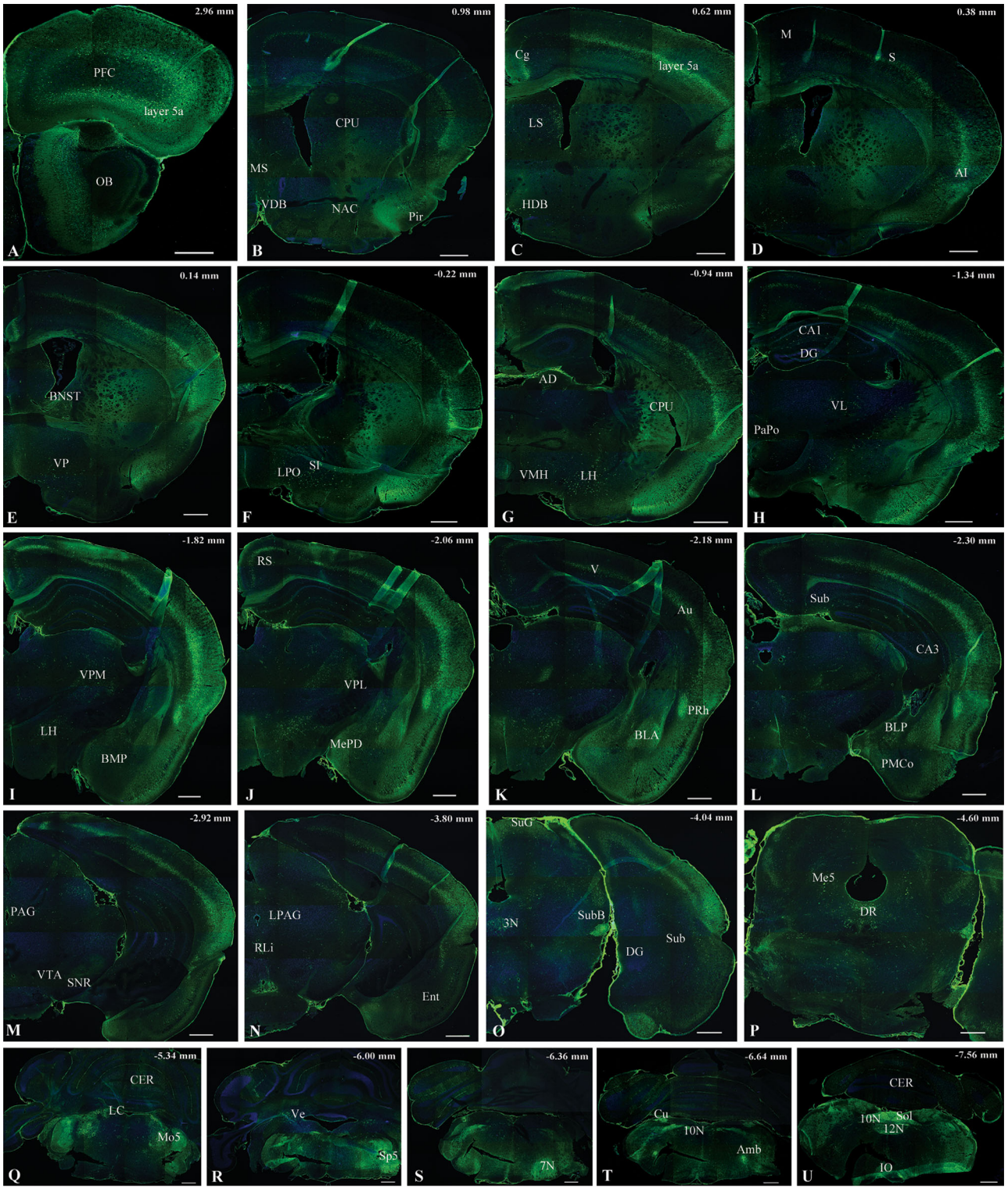

Figure 5. P11 expression throughout the whole brain revealed by immunocytochemistry with GFP antibody. The images represent selected plates from a series of semicoronal sections through the brain of the p11-EGFP transgenic mouse, presented in rostral to caudal order starting with the olfactory bulb **(A)** and ending with an image of the medulla and caudal cerebellum **(U)**. Approximate anatomical position of each image was determined using Paxinos and Franklin's *Mouse Brain in Stereotaxic Coordinates*. The coordinates as related to bregma are displayed at the top right corner of each image. Sections were from one brain, immunolabeled in one experiment with GFP antibody, stained with the nuclear stain DAPI, to enable the delineation between anatomical regions, and imaged with a confocal microscope. Abbreviations for representative structures are the same as in Table 2. Scale bars = 500 μ.

innervation (Figs. 3D, 8H, Movie S2), as well as the majority of brainstem cranial nuclei (Movie S2).

The in situ data, shown in Figures 6 and 7, were generated by hybridization with a p11-specific probe in a p11-EGFP mouse brain. The specificity of the probe was confirmed by the total lack of signal in a mouse with complete knockout of p11 (p11-KO), shown in Figure 6. The gross anatomical expression of p11 mRNA, revealed by hybridization signal, shows the same pattern of expression as the GFP immunoreactivity corresponding to the p11 protein. This further confirms that the p11-EGFP mouse line is suitable to use for detection of native p11. However, in a few areas the intensity of the hybridization and GFP staining do not match (Figs. 5, 7). For example, the claustrum and insular cortical areas, and the tegmental nuclei in the midbrain, are among the areas with higher in situ signal, while GFP has higher expression in layer 5a, striatum, some amygdalar, basal forebrain, hypothalamic, and brainstem nuclei. However, the most prominent difference is in the thalamus, where we observed stronger GFP staining in all areas (Figs. 5, 7).

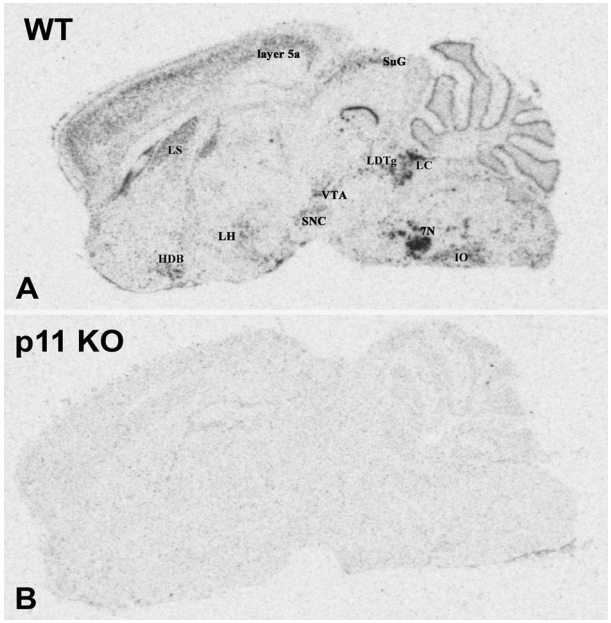

Figure 6. Conformation of the specificity of p11 probe. The hybridization signal in the sagittal section of a wildtype mouse (**A**) shows strong signal, while the corresponding section of a p11-knockout mouse (**B**) does not.

Whole-mount immunolabeling and volume imaging of the p11-EGFP transgenic mouse brain

While immunocytochemistry on tissue sections provides fine details on the cellular level, whole-tissue imaging affords a view of the expression patterns on the organ level. Volume imaging of the p11-GFP transgenic mouse brain matches the expression pattern observed in sections (Movies S1, S2). This analysis persuasively shows the relative abundance of GFP + cells, as well as intensity of the signal in different regions of the brain. GFP + cells with the most intense signal were detected in the cerebral cortex and brain stem regions, consistent with the data obtained by immunolabeling and in situ hybridization on tissue sections. However, the intensity of GFP staining in the meninges, ependymal cells, and blood vessel walls was much more prominent in iDISCO samples (Movie S3). This method also allows easier tracing of axonal tracts, such as the axon tracts in medulla (Movie S2). Furthermore, the distribution of blood vessels, with strong signal in the blood vessel walls, is better appreciated in volume imaging. For example, the gross anatomical distribution of the vasculature in hippocampus and specifically dentate gyrus is evident; blood vessels enter from the granule cell layer and once in the hilus they branch and form a dense vasculature network (Movie S3). In summary, iDISCO analysis of the GFP expression in the p11-EGFP mouse line together with the classical immunolabeling of tissue sections provide a detailed anatomical mapping of p11 expression in the brain.

P11 is expressed in nonneuronal cells within the brain

In addition to expression in multiple neuronal cell types, p11 is known to be expressed in cells in blood vessel walls and meninges (Fig. 2). Here we detected GFP immunoreactivity in nonneuronal cell types that morphologically resemble glia-like cells (Fig. 2E), and ependymal and the choroid plexus cells (Fig. 2F). We sought to confirm the subtype of glia by immunocytochemical analysis with various cell-specific markers on the sections from p11-EGFP and p11-TRAP mice lines using the antibodies listed in Table 1.

Immunolabeling with the astrocyte-specific markers aldehyde dehydrogenase 1-like, type 1 (Aldh1L1) and glial fibrillary acidic protein (GFAP) revealed that GFP + cells colabel with these astrocyte markers (Fig. 9A1–4). In addition, microglial marker Iba1 was colocalized with GFP + cells (Fig. 9B1–4), verifying that microglia express p11 in vivo. Oligodendrocyte markers Olig2 and CNPase, which label precursor and mature oligodendrocytes, respectively, did not label GFP + cells (data not shown). However, NG2, a marker of oligodendrocyte precursors, is expressed by a small population of GFP + cells in white matter tracts (Fig. 9C1–4).

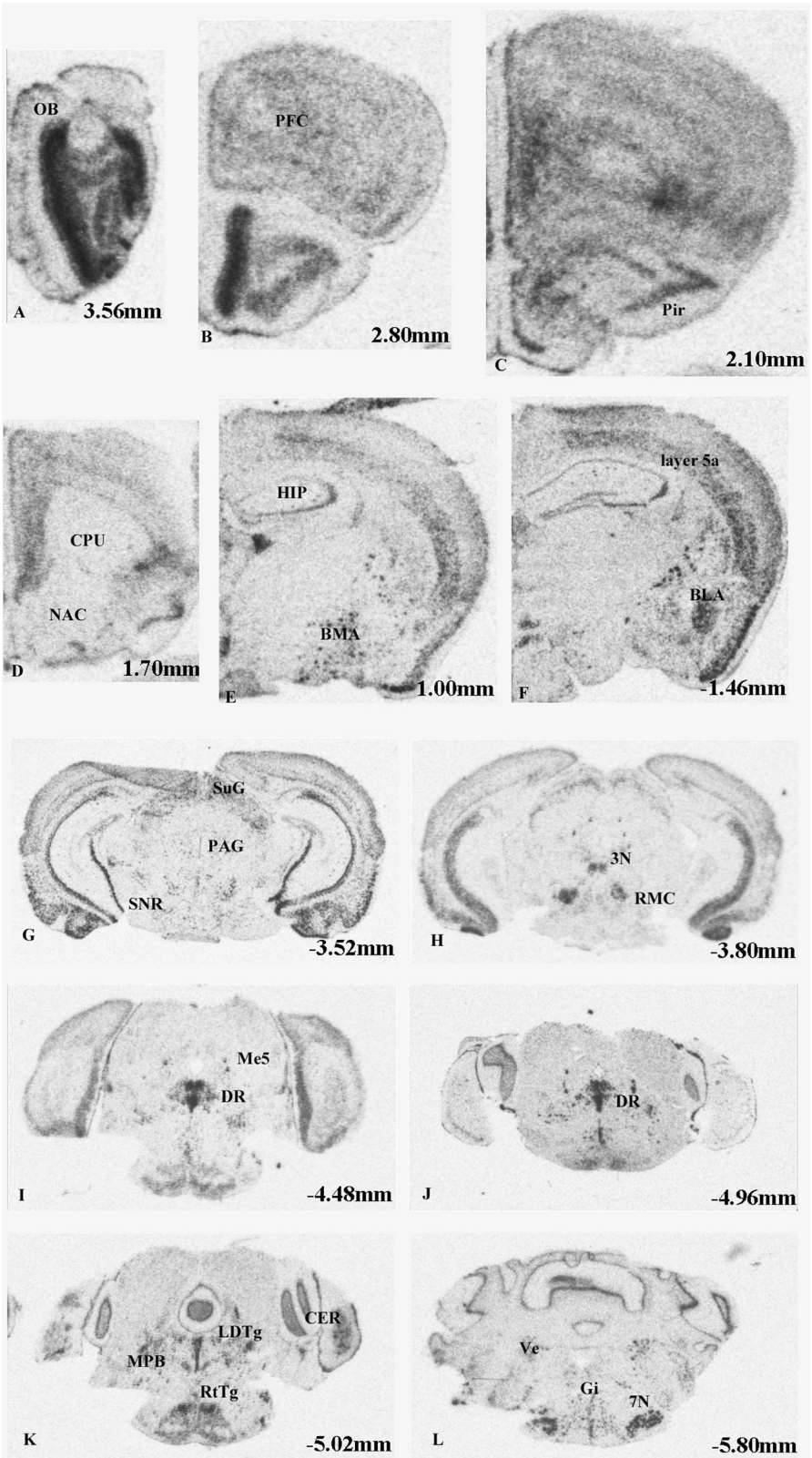

Figure 7. P11 expression revealed by in situ hybridization with p11-specific probe. The images are selected from serial sections cut coronally through the brain, rostral **(A)** to caudal **(L)**, representing the endogenous p11 mRNA in the brain of a wildtype mouse. Each image was chosen to correlate to the selected images showing GFP expression. Abbreviations for representative structures are the same as in Table 2.

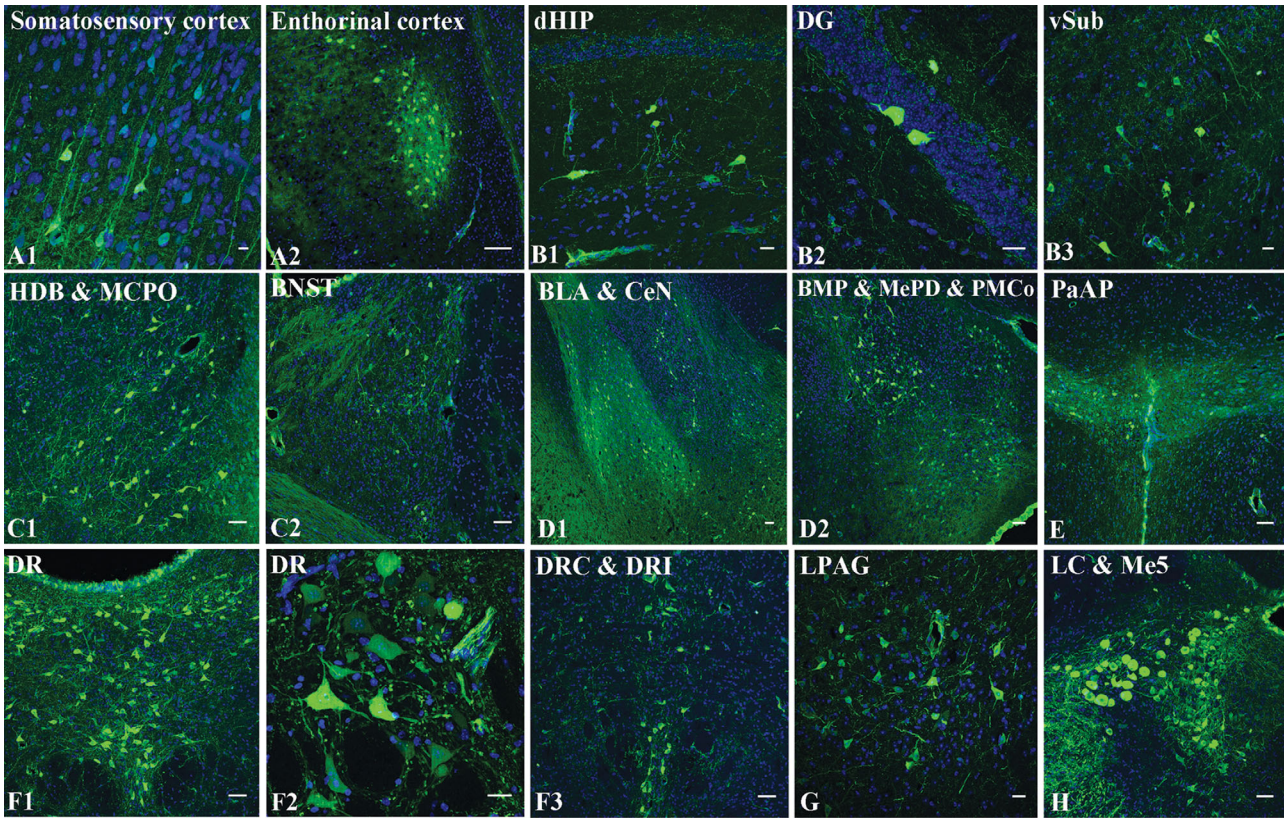

Figure 8. Representative images of the brain regions containing GFP + neurons. All images were obtained by imaging tissue sections from a p11-EGFP mouse immunolabeled with anti-GFP antibody (green) and counterstained with DAPI (blue). **(A1)** Layer 5a pyramidal neurons in the somatosensory cortex (lower left side of the image) have high GFP immunoreactivity, while scattered cells in layers 4 and 3 display lower GFP immunoreactivity signal. **(A2)** Strong signal is observed in layer 4/5 neurons of the dorsolateral entorhinal cortex (Ent). **(B1–3)** Expression of GFP in the dorsal hippocampus (dHIP) shows a small number of interneurons scattered in the molecular layer of CA1–3 regions (B1), basket cells in the dentate gyrus (DG), shown in B2. Subiculum, a part of the hippocampal formation, expresses GFP in pyramidal neurons and scattered interneurons only in the ventral hippocampus (B3). **(C1–2)** Basal forebrain contains scattered neurons with strong GFP immunoreactivity in several nuclei, including nucleus of the horizontal limb of the diagonal band-HDB, and magnocellular preoptic nucleus-MCPO (C1), as well as in bed nucleus of the stria terminalis (BNST), shown in C2. **(D1–2)** Representative images of the expression in amygdala: (D1) Basolateral amygdaloid nucleus (BLA) and central amygdaloid nucleus (CeN), and (D2) basomedial amygdaloid nucleus (BMP), medial amygdaloid nucleus (MePD) and posteromedial cortical amygdaloid nucleus (PMCo) all have strong expression in a subset of neurons. **(E)** Hypothalamic expression is represented by lateral paraventricular hypothalamic nucleus (PaAP), a posterior part of the hypothalamus-pituitary-adrenal axis. **(F1–3)** Dorsal raphe nuclei (DR) contain large number of GFP + cells in the ventral, dorsal, and lateral parts (F1,F3), as well as in dorsal raphe caudal (DRC) and interfascicular nuclei (DRI). Higher magnification of the DR shows that neurons show varying levels of GFP immunoreactivity (F2). **(G)** Scattered cells are also found in the lateral periaqueductal gray area (LPAG). **(H)** Locus coeruleus (LC) and mesencephalic trigeminal nucleus (Me5) contain large neurons with very strong GFP signal. Scale bars = 20 μ in A1,B1–3,F2,G; 100 μ in A2; 50 μ in C1–2,D1–2,E,F1,3,H.

Endothelial cells express p11 and we confirmed that GFP + cells were labeled with CD31 and von Willebrandt factor (data not shown), markers of endothelial cells (Asahara et al., 1997; Hess et al., 2004). Volume labeling (Movie S3) suggests that a large number of endothelial cells are GFP+, which is not apparent on the tissue sections. Furthermore, we sought to determine if p11 expression is confined to endothelial cells or if it extends to pericytes by applying the pericyte-specific markers alpha smooth muscle actin and platelet-derived growth factor receptor beta (Makihara et al., 2015). We used both mouse lines for this analysis, because the p11-TRAP line provides better cellular resolution for GFP + cells. All GFP + cells in blood vessel walls were colabeled with both endothelial and pericyte markers, regardless of the vessel size (data not shown), suggesting that both cell types express p11.

Furthermore, the brain parenchyma is lined with p11-expressing cells. Both ependymal cells, lining the ventricles throughout the brain (Fig. 2F1,2), and the meninges (Fig. 2H1–4), which envelop the brain, express high levels of GFP. Some of these GFP + cells are

endothelial cells from the blood vessels in the meninges, but the majority are meningeal cells. A small subset of cells in the choroid plexus are also GFP + (Fig. 2F1,2).

DISCUSSION

Gene expression databases showed a widespread expression of p11 in the mouse brain. The results presented here confirm the widespread distribution of this protein. We detected p11 in neurons and nonneuronal cells in distinct brain regions throughout the brain. Expression in nonneuronal cell types is widespread, while neuronal expression is region-specific and often restricted to a subset of neurons within each structure. Nonneuronal cell types that express p11 include three subtypes of glia, and endothelial, ependymal, choroid plexus, and meningeal cells. We also found that the expression levels vary between brain regions and cell types, in which some areas/cell types, such as neurons in the brainstem nuclei appear highly enriched, while other brain areas, such as basomedial amygdaloid nuclei, have considerably lower expression.

MDD is a disorder affecting multiple brain regions and cell types that are connected by intricate networks and include multiple neurotransmitter systems (Krishnan and Nestler, 2008; Price and Drevets, 2010). Given this complexity, the inquiry into the pathophysiology of depression should focus both on the cellular mechanisms as well as the anatomical and functional connectivity between brain regions and the whole organism. This approach has been demonstrated by the discovery of the molecular interactions between p11 and serotonergic receptors that contributes to the depressive-like phenotype of constitutive p11-KO mice (Svenningsson et al., 2006). The mechanism of p11 action has been investigated in mice (Svenningsson et al., 2006; Egeland et al., 2010; Warner-Schmidt et al., 2012; Oh et al., 2013; Lee et al., 2015)), followed by gene expression studies in MDD patients (Svenningsson et al., 2006, 2013; Zhang et al., 2008; Alexander et al., 2010). While our understanding of p11 actions on the systems level is increasing, only a subset of the neuronal cell types and brain regions have been investigated. To fully understand the role of p11 in these processes, a thorough mapping of p11 expression in the brain is essential. Here we provide comprehensive p11 expression data that includes a detailed anatomical map, generated using immunocytochemistry, in situ hybridization, and iDISCO volume imaging. Furthermore, we confirmed the expression in nonneuronal cell types and determined glial subtypes that express p11.

It is noteworthy that the results obtained using multiple detection techniques match well, and the discrepancies can be explained by alterations in sensitivity on the cellular level, as well as the different methods used. For example, Oh et al. (2013) did not detect p11-expressing glial cells in the hippocampus, while Warner-Schmidt et al. (2011) indicate expression in glia, although without further analysis. Confirming our and Warner-Schmidt et al.'s expression data obtained with various methods, such as array analysis (Zhang et al., 2014) and RNA sequencing (J.P. Roussarie and A. Milosevic, pers. commun.), we found expression of p11 in glial cells. It has been reported that different mouse strains have variable levels of p11 expression (Zimmer et al., 2005), and thus the expression level in each cell type may vary between different strains, prompting slightly different protein content and consequently the immunostaining results. However, we did not detect differences in GFP immunoreactivity between two strains of mice, CD1 and C57BL/6, used in this study. Thus, present discrepancies in immunoreactivity on the cellular level are most likely a result of slight variability in immunolabeling protocol, such as concentration of the fixative and the thickness of tissue sections used. In summary, we detected p11 in neurons in 80 distinct areas in the brain, as well as in three types of glial cells: endothelial, ependymal, and meningeal cells. Furthermore, the immunoreactivity in iDISCO volume imaging appears slightly different, most notably in blood vessels and meninges. This is probably caused by projection images from cleared tissues that enhance the larger or densely labeled structures when they are summed over thick optical sections of tissue. Similar images from standard confocal methods of nontransparent preparations inherently reveal cross-sections of the structures due to limited optical penetration. The example of a blood vessel will appear merely as a ring in a confocal image, whereas a continuous cylinder from the transparent tissue is strikingly brighter. In addition, the GFP expression is not expected to leak out of cells and relocate to vessels and endothelial cells. This is evident in the staining of other GFP mouse models (glial- and ChAT-GFP transgenic mice were extensively tested, T. Liebmann, pers. commun.), where we do not see enriched immunoreactivity in vessels and endothelial cells.

Regional specificity of the P11 mechanism of action

At present, the role of p11 has been investigated in cortical layer 5a, the nucleus accumbens, and the dentate gyrus of the hippocampus. We have shown that

other areas implicated in depression display strong p11 mRNA expression, as well as GFP expression in a subset of their neurons. These areas include the nuclei of the basal forebrain, basolateral amygdala, and brainstem monoaminergic nuclei. These regions are extremely important in the neuronal circuitry underlying numerous psychiatric diseases (Price and Drevets, 2012), but the role of p11 remains to be elucidated. For example, the distribution and morphology of p11 + cells in the basal forebrain suggest expression in cholinergic neurons, similar to those in the nucleus accumbens. Dysfunction of the cholinergic connectivity between the basal forebrain and cortex has been extensively studied (for review, see Drevets et al., 2008; Sarter, 2008; Price and Drevets, 2012). While the role of p11 in choline acetyltransferase (ChAT) cells in the nucleus accumbens has been elucidated (Warner-Schmidt et al., 2012; Virk et al., 2016), p11 signaling in the basal forebrain may be different, since these are projection neurons and their circuitry differs from the accumbal ChAT interneurons.

Next, the amygdala is known to regulate anxiety via microcircuitry between the basolateral and central amygdaloid nuclei (Tye et al., 2011; Tye and Deisseroth, 2012), and fear conditioning via connections to the prefrontal cortex and basal amygdala (Senn et al., 2014). Molecular mechanisms and circuitry of p11 + cells in the amygdala are not known at present, but the strong signal in the basolateral amygdaloid nucleus would suggest a possible role in anxiety symptoms present in MDD.

Several areas in the hypothalamus have strong p11 expression. For example, the lateral hypothalamus p11 + cells have been shown to secrete orexin/hypocretin and project to the nucleus accumbens and it has been suggested that they may regulate behavior related to specific symptoms of depression, such as abnormal food intake (Ekstrand et al., 2014). Moreover, p11 may have a role in regulating the stress response, since it is expressed in the paraventricular hypothalamic nucleus. This brain region contains cells that secrete oxytocin and vasopressin, as well as corticotropin-releasing hormone, and has a critical role in hypothalamo-pituitary-adrenal stress response (Jankord and Herman, 2008).

Notably, p11 expression was detected in several monoaminergic nuclei in the brainstem. Monoamines, which include serotonin, dopamine, and noradrenaline, regulate mood, food intake, learning and memory, locomotion, sleep, and many other processes. Altered levels of monoamines and changes in signaling have long been considered as one of possible causes of MDD, and are currently the basis for treatment with serotonin or noradrenaline reuptake inhibitors and monoamine oxidase inhibitors (Chaudhury et al., 2015). Dorsal raphe, the largest serotonergic nuclei in the brain, contain neurons that express p11 at a very high level. The role of p11 in the functioning of the dorsal raphe neurons remains to be examined, but the data from our laboratory would suggest a role in regulating serotonergic signaling, gene expression, and serotonin secretion, possibly via interaction with the 5HT1b serotonergic receptor, which serves as an autoreceptor on serotonin neurons (P. Svenningsson, pers. commun.) The three distinct regions of the midbrain dopaminergic system, the substantia nigra, ventral tegmental area, and retrorubral field, as well as the noradrenergic locus coeruleus vary in their p11 expression. The biological importance of such differential expression is not clear. These nuclei play very important roles in depressive behavior (Chaudhury et al., 2013; Lammel et al., 2014), and second-generation antidepressants target monoaminergic systems (Hillhouse and Porter, 2015). However, the role of p11 is most likely not related specifically to dopamine or noradrenaline, since the current literature does not indicate an interaction of p11 with dopaminergic or noradrenergic receptors, or regulation of neurotransmitters' transcription, synthesis, and secretion. Thus, it is more likely that the distinct connectivity of each nucleus, including receptors and cotransmitters expressed by each neuronal subtype, define the role of p11 in these regions, similar to regulation of the accumbal ChAT activity (Virk et al., 2016).

Our data and the literature point to multiple roles of p11 in cellular processes and in order to elucidate the mechanism of p11 action in MDD, brain regions important for the etiology of MDD should be examined. This approach has been used successfully in recent studies in which it was found that p11 has different roles in depressive-like behaviors, depending on the region and cell type. Cortical layer 5a pyramidal neurons (Schmidt et al., 2012), ChAT neurons in the nucleus accumbens (Warner-Schmidt et al., 2012), and mossy cells in the hippocampus (Oh et al., 2013) all have higher GFP immunoreactivity relative to other cells in these regions. However, deletion of p11 in ChAT cells in the nucleus accumbens induces anhedonia and despair in mice (Warner-Schmidt et al., 2012), while deletion in the cingulate cortex, known to have a major role in psychiatric disorders (Drevets et al., 2008; Price and Drevets, 2012), fails to induce depression-like behavior (Alexander et al., 2010). Nevertheless, when p11 is deleted from all forebrain glutamatergic neurons, not only those in the cingulate cortex, mice became susceptible to depression upon being exposed to a mild stressor (Lee et al., 2015). The response to antidepressants is also region-specific, so deletion of p11 specifically in

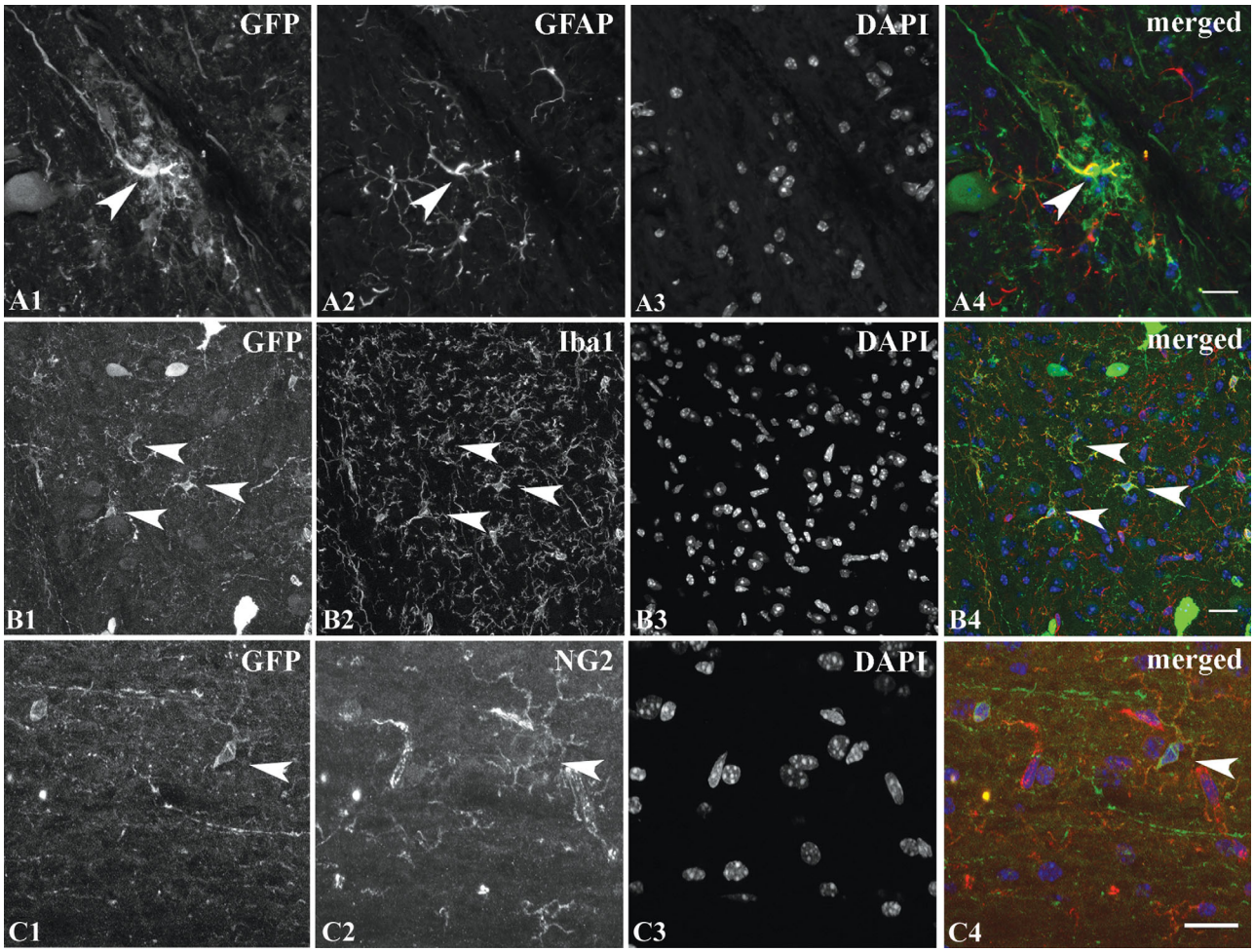

Figure 9. GFP is expressed in three subtypes of glial cells. Characterization of glial subtypes was performed using subtype-specific antibodies on the sections from the p11-EGFP line. Row **(A1–4)** Astrocyte in the white matter tract in the medulla (arrowhead) is labeled with the astrocyte marker GFAP (red) and GFP (green) antibodies. Row **(B1–4)** Microglial marker Iba1 (blue) colabels GFP (green) cells (arrowheads), but not neurons immunolabeled with the NeuN antibody (red). Row **(C1–4)** Small glial cell (arrowhead) in the corpus callosum colabeled with anti-GFP (green) and neural/glial antigen 2 NG2 (red), the marker of pluripotent glial cells and oligodendrocyte progenitors. Scale bars = 20 μ.

accumbal ChAT cells does not affect the response to antidepressants (Warner-Schmidt et al., 2012), while the antidepressant action is abolished after deleting p11 from cortical layer 5a (Schmidt et al., 2012). These results suggest that multiple brain regions are involved in the etiology of MDD and underline the region specificity of the p11-dependent mechanism of action and antidepressant response.

It is also interesting to note that the number of p11 cells within each region is not critical for key effects on behavior. For example, cholinergic p11 + cells in the nucleus accumbens encompass between one and two percent of total cells in this region, yet deletion of p11 specifically in these cells has a profound effect on depressive behaviors (Warner-Schmidt et al., 2012), while deletion of p11 in a large number of p11 + cells in layer 5a of the prefrontal or cingulate cortex does not (Alexander et al., 2010; Schmidt et al., 2012).

Although an emphasis of these studies has been on the areas of the brain with a clear role in depression, it is interesting to note that the nuclei of the cranial nerves in the brainstem have the highest level of p11 expression across all brain regions. This suggests a key role that p11 may have in regulating vital body functions, such as transmission of sensory information, and visceral, cardiac, and respiratory functions. However, the role of p11 in these neurons remains unknown. Does it involve localization of receptors other then those for serotonin and thus help communication between the brain and the rest of the body? The main neurotransmitter in some of these nuclei is acetylcholine, but there is also dense serotonergic innervation in

this area (www.gensat.org). Recently, it has been reported that p11 regulates calcium signaling and excitation-contraction coupling in cardiomyocites via 5-HT4 receptor signaling (Meschin et al., 2015). It may be possible that p11 has a similar mechanisms of action in neurons of the cranial nuclei.

Together, the results presented here show that GFP immunolabeling, substituting for p11 expression, encompasses many brain regions and colocalizes with the major outputs for glutamatergic, cholinergic, dopaminergic, noradrenergic, and serotonergic innervation and neuromodulators such as vasopressin, corticotropin-releasing hormone, and hypocretin. In addition, p11 is expressed in some types of GABAergic neurons, but not the others (Heiman et al., 2008; Schmidt et al., 2012). These regions play key roles in regulating a wide variety of behaviors, including emotional and stress responses, learning and memory, and motor functions. Thus, widespread expression of p11 results in a complex role in brain functioning on the cellular and organ level. One way to parse out this complexity is to characterize regional and cellular differences in p11 actions.

Cellular mechanisms of p11 action depend on circuitry

Regional specificity of p11 actions may be instigated by a unique combination of different neurotransmitter receptors and ion channels expressed in neuronal subtypes found in different brain regions. It was shown that p11 stabilizes serotonergic receptors on the cell membrane, thus regulating the cellular response to the neurotransmitter (Svenningsson et al., 2006). However, each cell type expresses a unique subset of serotonergic receptors (Egeland et al., 2011; Schmidt et al., 2012; Warner-Schmidt et al., 2012; Eriksson et al., 2013), and therefore the behavioral outcome of perturbed p11-dependant signaling depends on the specific subtype of serotonergic receptor expressed.

P11 interaction with other neurotransmitter receptors, such as the recently described metabotropic glutamate receptor mGluR5 on glutamatergic neurons, also appears to be involved in regulation of processes underlying depression (Lee et al., 2015). This may be especially relevant for the areas where glutamate is the predominant neurotransmitter, such as the cortex and amygdala. Furthermore, p11 is involved in trafficking of various ion channels, including the voltage-gated sodium channel $Na_V1.8$ (Okuse et al., 2002), acid-sensing ion channel (Donier et al., 2005), and TASK-1 potassium channel (Girard et al., 2002; Renigunta et al., 2006). The deletion of p11 from primary sensory neurons abolishes the response to noxious pain due to the deficit in trafficking of $Na_V1.8$, showing the importance of p11 in the functioning of the peripheral nervous system (Foulkes et al., 2006). Taken together, these data suggest that p11 interacts with receptors and channels of other neurotransmitter systems in addition to serotonin, and has a complex role in MDD.

Additional complexity of p11 action involves regulation of gene transcription. P11 is a key component of the cellular signaling cascade that activates gene transcription by interacting with the chromatin regulator SMARCA3 (Oh et al., 2013). While this was demonstrated in the mossy and basket cells of the dentate gyrus, it remains to be examined if this same mechanism of action applies for other cell types that contain p11.

A first step towards understanding the mechanism of p11 action in different brain regions would be determining the molecular profile of each p11 + neuronal subtype. Currently, their precise molecular profile in the majority of brain regions involved in depression remains unknown. The characterization of the specific subtypes of the p11 + neurons was beyond the scope of this study, but our current knowledge of the cellular and molecular mechanism of MDD warrants the analysis of their gene expression and connectivity in regions relevant to depression.

Role of p11 in nonneuronal cells

P11 was initially detected in various tissues by western blot analysis, and mapping in the brain was done by in situ hybridization (Zimmer et al., 2005; Svenningsson et al., 2006). Neither of these techniques can provide information about the specific cell types that express p11. In this study we used immunocytochemical labeling with antibodies against glial markers and found p11 in astrocytes, microglia, and a subset of oligodendrocytes. As opposed to neurons, where even within the same structure only a subset of neurons expresses p11, p11 + astrocytes and microglia are widespread. Restricted glial expression was found only in the white matter tracts where a subset of oligodendrocyte progenitors, also known as NG2 cells (Nishiyama et al., 1999), express p11. To our knowledge, the presence of p11 protein in glial cells in the healthy brain has not been reported previously. However, it is known that reactive astrocytes in an injured brain upregulate expression of p11 (Zamanian et al., 2012). In addition, p11 transcripts were found in multiple glial cell types, including mature oligodendrocytes and microglia, in ex vivo conditions (Zhang et al., 2014).

At present, the role of glial cells in depression is well established. The number and morphology of glial cells

are changed in MDD patients and in animal models (Czeh et al., 2006; Rajkowska and Miguel-Hidalgo, 2007; Banasr and Duman, 2008; Lee and Fields, 2009; Liu et al., 2012; Oh et al., 2012; Birey et al., 2015). Gene expression analyses have shown that glial genes, including those involved in the glutamate cycle, inflammation, and structural components of myelin, are very often changed in key brain areas such as prefrontal cortex and hippocampus (Aston et al., 2005; Choudary et al., 2005; Bernard et al., 2011). Neuroinflammation as a cause of depression gained attention recently, supported by a body of evidence that MDD patients have high levels of multiple inflammatory markers and that cytokines induce a depressive-like state (Krishnan and Nestler, 2008; Dowlati et al., 2010; Warner-Schmidt et al., 2011; Russo and Nestler, 2013; Hodes et al., 2015). These active molecules enter the brain parenchyma through the blood–brain barrier, comprised of the endothelial cells and astrocytes (Abbott et al., 2006), and the structure and permeability of the blood–brain barrier is changed in depression (Najjar et al., 2013; Rajkowska et al., 2013). However, the role of p11 in these cells is not known, especially in the context of MDD, and remains to be examined.

SUMMARY

We have provided a comprehensive p11 expression atlas that includes regional and cell specificity. With such widespread expression, it is necessary to elucidate the mechanisms of action in each cell type, as well as their connectivity with other brain regions, to fully understand the role of p11 in depression and other mood disorders.

ACKNOWLEDGMENTS

We thank Drs. Eric Schmidt and Nathaniel Heintz for a generous gift of the S100a10 bacTRAP mouse line. We thank Dr. Alison North at the Rockefeller Bioimaging Resource Center for help with confocal microscopy and Dr. Katia Manova-Todorova, Yevgeniy Romin, and Sho Fujisava at the Molecular Cytology Core at the Memorial Sloan Kettering Cancer Center for help with the imaging on the Mirax Scan. The authors thank Elizabeth Griggs for expert help with graphics. Special thanks to Dr. Laura Kus for expert help with anatomical characterization of expression structures. We thank Drs. Yong Kim, Yotam Sagi, Yong-Seok Oh, and Jean-Pierre Roussarie who read the article and offered thoughtful suggestions.

CONFLICT OF INTEREST

The authors declare no conflicts of interest.

ROLE OF AUTHORS

All authors take responsibility for the accuracy of the data and analysis. All authors had full access to all the data in the study. Study concept and design: AM, PG, PS. Acquisition of the data: AM, TL, MK, NS. Analysis and interpretation of the data: AM, TL, PS, PG. Drafting of the article: AM, TL, MK, PS. Critical revision of the article: AM, PG, PS. Obtained funding: PS, PG. Technical support: MK, NS. Study supervisor: AM, PG.

LITERATURE CITED

Abbott NJ, Ronnback L, Hansson E. 2006. Astrocyte-endothelial interactions at the blood-brain barrier. Nat Rev Neurosci 7:41–53.

Alexander B, Warner-Schmidt J, Eriksson T, Tamminga C, Arango-Lievano M, Ghose S, Vernov M, Stavarache M, Musatov S, Flajolet M, Svenningsson P, Greengard P, Kaplitt MG. 2010. Reversal of depressed behaviors in mice by p11 gene therapy in the nucleus accumbens. Sci Transl Med 2:54ra76.

Anisman H, Du L, Palkovits M, Faludi G, Kovacs GG, Szontagh-Kishazi P, Merali Z, Poulter MO. 2008. Serotonin receptor subtype and p11 mRNA expression in stress-relevant brain regions of suicide and control subjects. J Psychiatry Neurosci 33:131–141.

Asahara T, Murohara T, Sullivan A, Silver M, van der Zee R, Li T, Witzenbichler B, Schatteman G, Isner JM. 1997. Isolation of putative progenitor endothelial cells for angiogenesis. Science 275:964–967.

Aston C, Jiang L, Sokolov BP. 2005. Transcriptional profiling reveals evidence for signaling and oligodendroglial abnormalities in the temporal cortex from patients with major depressive disorder. Mol Psychiatry 10:309–322.

Babiychuk EB, Draeger A. 2000. Annexins in cell membrane dynamics. Ca(2+)-regulated association of lipid microdomains. J Cell Biol 150:1113–1124.

Banasr M, Duman RS. 2008. Glial loss in the prefrontal cortex is sufficient to induce depressive-like behaviors. Biol Psychiatry 64:863–870.

Bang SJ, Commons KG. 2012. Forebrain GABAergic projections from the dorsal raphe nucleus identified by using GAD67-GFP knock-in mice. J Comp Neurol 520:4157–4167.

Benton RL, Maddie MA, Minnillo DR, Hagg T, Whittemore SR. 2008. Griffonia simplicifolia isolectin B4 identifies a specific subpopulation of angiogenic blood vessels following contusive spinal cord injury in the adult mouse. J Comp Neurol 507:1031–1052.

Bernard R, Kerman IA, Thompson RC, Jones EG, Bunney WE, Barchas JD, Schatzberg AF, Myers RM, Akil H, Watson SJ. 2011. Altered expression of glutamate signaling, growth factor, and glia genes in the locus coeruleus of patients with major depression. Mol Psychiatry 16:634–646.

Birey F, Kloc M, Chavali M, Hussein I, Wilson M, Christoffel DJ, Chen T, Frohman MA, Robinson JK, Russo SJ, Maffei A, Aguirre A. 2015. Genetic and stress-induced loss of NG2 glia triggers emergence of depressive-like behaviors through reduced secretion of FGF2. Neuron 88:941–956.

Chaudhury D, Walsh JJ, Friedman AK, Juarez B, Ku SM, Koo JW, Ferguson D, Tsai HC, Pomeranz L, Christoffel DJ, Nectow AR, Ekstrand M, Domingos A, Mazei-Robison MS, Mouzon E, Lobo MK, Neve RL, Friedman JM, Russo SJ, Deisseroth K, Nestler EJ, Han MH. 2013. Rapid

regulation of depression-related behaviours by control of midbrain dopamine neurons. Nature 493:532–536.
Chaudhury D, Liu H, Han MH. 2015. Neuronal correlates of depression. Cell Mol Life Sci 72:4825–4848.
Chen J, Condron BG. 2009. Drosophila serotonergic varicosities are not distributed in a regular manner. J Comp Neurol 515:441–453.
Choudary PV, Molnar M, Evans SJ, Tomita H, Li JZ, Vawter MP, Myers RM, Bunney WE Jr, Akil H, Watson SJ, Jones EG. 2005. Altered cortical glutamatergic and GABAergic signal transmission with glial involvement in depression. Proc Natl Acad Sci U S A 102:15653–15658.
Czeh B, Simon M, Schmelting B, Hiemke C, Fuchs E. 2006. Astroglial plasticity in the hippocampus is affected by chronic psychosocial stress and concomitant fluoxetine treatment. Neuropsychopharmacology 31:1616–1626.
Dassah M, Deora AB, He K, Hajjar KA. 2009. The endothelial cell annexin A2 system and vascular fibrinolysis. Gen Physiol Biophys 28(Spec No Focus):F20–28.
Donier E, Rugiero F, Okuse K, Wood JN. 2005. Annexin II light chain p11 promotes functional expression of acid-sensing ion channel ASIC1a. J Biol Chem 280:38666–38672.
Dougherty JD, Fomchenko EI, Akuffo AA, Schmidt E, Helmy KY, Bazzoli E, Brennan CW, Holland EC, Milosevic A. 2012. Candidate pathways for promoting differentiation or quiescence of oligodendrocyte progenitor-like cells in glioma. Cancer Res 72:4856–4868.
Dowlati Y, Herrmann N, Swardfager W, Liu H, Sham L, Reim EK, Lanctot KL. 2010. A meta-analysis of cytokines in major depression. Biol Psychiatry 67:446–457.
Doyle JP, Dougherty JD, Heiman M, Schmidt EF, Stevens TR, Ma G, Bupp S, Shrestha P, Shah RD, Doughty ML, Gong S, Greengard P, Heintz N. 2008. Application of a translational profiling approach for the comparative analysis of CNS cell types. Cell 135:749–762.
Drevets WC, Price JL, Furey ML. 2008. Brain structural and functional abnormalities in mood disorders: implications for neurocircuitry models of depression. Brain Struct Funct 213:93–118.
Egeland M, Warner-Schmidt J, Greengard P, Svenningsson P. 2010. Neurogenic effects of fluoxetine are attenuated in p11 (S100A10) knockout mice. Biol Psychiatry 67:1048–1056.
Egeland M, Warner-Schmidt J, Greengard P, Svenningsson P. 2011. Co-expression of serotonin 5-HT(1B) and 5-HT(4) receptors in p11 containing cells in cerebral cortex, hippocampus, caudate-putamen and cerebellum. Neuropharmacology 61:442–450.
Ekstrand MI, Nectow AR, Knight ZA, Latcha KN, Pomeranz LE, Friedman JM. 2014. Molecular profiling of neurons based on connectivity. Cell 157:1230–1242.
Eriksson TM, Alvarsson A, Stan TL, Zhang X, Hascup KN, Hascup ER, Kehr J, Gerhardt GA, Warner-Schmidt J, Arango-Lievano M, Kaplitt MG, Ogren SO, Greengard P, Svenningsson P. 2013. Bidirectional regulation of emotional memory by 5-HT1B receptors involves hippocampal p11. Mol Psychiatry 18:1096–1105.
Fortin GM, Bourque MJ, Mendez JA, Leo D, Nordenankar K, Birgner C, Arvidsson E, Rymar VV, Berube-Carriere N, Claveau AM, Descarries L, Sadikot AF, Wallen-Mackenzie A, Trudeau LE. 2012. Glutamate corelease promotes growth and survival of midbrain dopamine neurons. J Neurosci 32:17477–17491.
Foulkes T, Nassar MA, Lane T, Matthews EA, Baker MD, Gerke V, Okuse K, Dickenson AH, Wood JN. 2006. Deletion of annexin 2 light chain p11 in nociceptors causes deficits in somatosensory coding and pain behavior. J Neurosci 26:10499–10507.
Fricker-Gates RA, White A, Gates MA, Dunnett SB. 2004. Striatal neurons in striatal grafts are derived from both post-mitotic cells and dividing progenitors. Eur J Neurosci 19:513–520.
Gautier HO, Evans KA, Volbracht K, James R, Sitnikov S, Lundgaard I, James F, Lao-Peregrin C, Reynolds R, Franklin RJ, Karadottir RT. 2015. Neuronal activity regulates remyelination via glutamate signalling to oligodendrocyte progenitors. Nat Commun 6:8518.
Gerke V, Creutz CE, Moss SE. 2005. Annexins: linking Ca2 + signalling to membrane dynamics. Nat Rev Mol Cell Biol 6:449–461.
Girard C, Tinel N, Terrenoire C, Romey G, Lazdunski M, Borsotto M. 2002. p11, an annexin II subunit, an auxiliary protein associated with the background K + channel, TASK-1. EMBO J 21:4439–4448.
Gong S, Zheng C, Doughty ML, Losos K, Didkovsky N, Schambra UB, Nowak NJ, Joyner A, Leblanc G, Hatten ME, Heintz N. 2003. A gene expression atlas of the central nervous system based on bacterial artificial chromosomes. Nature 425:917–925.
Hayes MJ, Shao D, Bailly M, Moss SE. 2006. Regulation of actin dynamics by annexin 2. EMBO J 25:1816–1826.
Hedhli N, Falcone DJ, Huang B, Cesarman-Maus G, Kraemer R, Zhai H, Tsirka SE, Santambrogio L, Hajjar KA. 2012. The annexin A2/S100A10 system in health and disease: emerging paradigms. J Biomed Biotechnol 2012:406273.
Heiman M, Schaefer A, Gong S, Peterson JD, Day M, Ramsey KE, Suarez-Farinas M, Schwarz C, Stephan DA, Surmeier DJ, Greengard P, Heintz N. 2008. A translational profiling approach for the molecular characterization of CNS cell types. Cell 135:738–748.
Hess DC, Abe T, Hill WD, Studdard AM, Carothers J, Masuya M, Fleming PA, Drake CJ, Ogawa M. 2004. Hematopoietic origin of microglial and perivascular cells in brain. Exp Neurol 186:134–144.
Hillhouse TM, Porter JH. 2015. A brief history of the development of antidepressant drugs: from monoamines to glutamate. Exp Clin Psychopharmacol 23:1–21.
Hodes GE, Kana V, Menard C, Merad M, Russo SJ. 2015. Neuroimmune mechanisms of depression. Nat Neurosci 18: 1386–1393.
Jankord R, Herman JP. 2008. Limbic regulation of hypothalamopituitary-adrenocortical function during acute and chronic stress. Ann N Y Acad Sci 1148:64–73.
Justice NJ, Yuan ZF, Sawchenko PE, Vale W. 2008. Type 1 corticotropin-releasing factor receptor expression reported in BAC transgenic mice: implications for reconciling ligand-receptor mismatch in the central corticotropin-releasing factor system. J Comp Neurol 511:479–496.
Kim JY, Sun Q, Oglesbee M, Yoon SO. 2003. The role of ErbB2 signaling in the onset of terminal differentiation of oligodendrocytes in vivo. J Neurosci 23:5561–5571.
Krishnan V, Nestler EJ. 2008. The molecular neurobiology of depression. Nature 455:894–902.
Lammel S, Lim BK, Malenka RC. 2014. Reward and aversion in a heterogeneous midbrain dopamine system. Neuropharmacology 76(Pt B):351–359.
Le Bouffant F, Capdevielle J, Guillemot JC, Sladeczek F. 1998. Characterization of brain PCTAIRE-1 kinase immunoreactivity and its interactions with p11 and 14-3-3 proteins. Eur J Biochem FEBS 257:112–120.
Lee PR, Fields RD. 2009. Regulation of myelin genes implicated in psychiatric disorders by functional activity in axons. Front Neuroanat 3:4.
Lee KW, Westin L, Kim J, Chang JC, Oh YS, Amreen B, Gresack J, Flajolet M, Kim D, Aperia A, Kim Y, Greengard

P. 2015. Alteration by p11 of mGluR5 localization regulates depression-like behaviors. Mol Psychiatry 20:1546–1556.

Liu CY, Fraser SE, Koos DS. 2009. Grueneberg ganglion olfactory subsystem employs a cGMP signaling pathway. J Comp Neurol 516:36–48.

Liu J, Dietz K, DeLoyht JM, Pedre X, Kelkar D, Kaur J, Vialou V, Lobo MK, Dietz DM, Nestler EJ, Dupree J, Casaccia P. 2012. Impaired adult myelination in the prefrontal cortex of socially isolated mice. Nat Neurosci 15:1621–1623.

Madureira PA, O'Connell PA, Surette AP, Miller VA, Waisman DM. 2012. The biochemistry and regulation of S100A10: a multifunctional plasminogen receptor involved in oncogenesis. J Biomed Biotechnol 2012:353687.

Mai J, Finley RL Jr, Waisman DM, Sloane BF. 2000. Human procathepsin B interacts with the annexin II tetramer on the surface of tumor cells. J Biol Chem 275:12806–12812.

Makihara N, Arimura K, Ago T, Tachibana M, Nishimura A, Nakamura K, Matsuo R, Wakisaka Y, Kuroda J, Sugimori H, Kamouchi M, Kitazono T. 2015. Involvement of platelet-derived growth factor receptor beta in fibrosis through extracellular matrix protein production after ischemic stroke. Exp Neurol 264:127–134.

Menke M, Gerke V, Steinem C. 2005. Phosphatidylserine membrane domain clustering induced by annexin A2/S100A10 heterotetramer. Biochemistry 44:15296–15303.

Meschin P, Demion M, Cazorla O, Finan A, Thireau J, Richard S, Lacampagne A. 2015. p11 modulates calcium handling through 5-HTR pathway in rat ventricular cardiomyocytes. Cell Calcium 58:549–557.

Milosevic A, Goldman JE. 2002. Progenitors in the postnatal cerebellar white matter are antigenically heterogeneous. J Comp Neurol 452:192–203.

Milosevic A, Goldman JE. 2004. Potential of progenitors from postnatal cerebellar neuroepithelium and white matter: lineage specified vs. multipotent fate. Mol Cell Neurosci 26:342–353.

Milosevic A, Noctor SC, Martinez-Cerdeno V, Kriegstein AR, Goldman JE. 2008. Progenitors from the postnatal forebrain subventricular zone differentiate into cerebellar-like interneurons and cerebellar-specific astrocytes upon transplantation. Mol Cell Neurosci 39:324–334.

Najjar S, Pearlman DM, Devinsky O, Najjar A, Zagzag D. 2013. Neurovascular unit dysfunction with blood-brain barrier hyperpermeability contributes to major depressive disorder: a review of clinical and experimental evidence. J Neuroinflamm 10:142.

Nishiyama A, Chang A, Trapp BD. 1999. NG2 + glial cells: a novel glial cell population in the adult brain. J Neuropathol Exp Neurol 58:1113–1124.

Oh DH, Son H, Hwang S, Kim SH. 2012. Neuropathological abnormalities of astrocytes, GABAergic neurons, and pyramidal neurons in the dorsolateral prefrontal cortices of patients with major depressive disorder. Eur Neuropsychopharmacol 22:330–338.

Oh YS, Gao P, Lee KW, Ceglia I, Seo JS, Zhang X, Ahn JH, Chait BT, Patel DJ, Kim Y, Greengard P. 2013. SMARCA3, a chromatin-remodeling factor, is required for p11-dependent antidepressant action. Cell 152:831–843.

Okuse K, Malik-Hall M, Baker MD, Poon WY, Kong H, Chao MV, Wood JN. 2002. Annexin II light chain regulates sensory neuron-specific sodium channel expression. Nature 417:653–656.

Paxinos G, Franklin KBJ. 2004. The mouse brain in stereotaxic coordinates. Amsterdam, Boston: Elsevier Academic Press.

Price JL, Drevets WC. 2010. Neurocircuitry of mood disorders. Neuropsychopharmacology 35:192–216.

Price JL, Drevets WC. 2012. Neural circuits underlying the pathophysiology of mood disorders. Trends Cogn Sci 16:61–71.

Raff MC, Fields KL, Hakomori SI, Mirsky R, Pruss RM, Winter J. 1979. Cell-type-specific markers for distinguishing and studying neurons and the major classes of glial cells in culture. Brain Res 174:283–308.

Rajkowska G, Miguel-Hidalgo JJ. 2007. Gliogenesis and glial pathology in depression. CNS Neurol Disord Drug Targets 6:219–233.

Rajkowska G, Hughes J, Stockmeier CA, Javier Miguel-Hidalgo J, Maciag D. 2013. Coverage of blood vessels by astrocytic endfeet is reduced in major depressive disorder. Biol Psychiatry 73:613–621.

Renier N, Wu Z, Simon DJ, Yang J, Ariel P, Tessier-Lavigne M. 2014. iDISCO: a simple, rapid method to immunolabel large tissue samples for volume imaging. Cell 159:896–910.

Renier N, Adams EL, Kirst C, Wu Z, Azevedo R, Kohl J, Autry AE, Kadiri L, Umadevi Venkataraju K, Zhou Y, Wang VX, Tang CY, Olsen O, Dulac C, Osten P, Tessier-Lavigne M. 2016. Mapping of brain activity by automated volume analysis of immediate early genes. Cell 165:1789–1802.

Renigunta V, Yuan H, Zuzarte M, Rinne S, Koch A, Wischmeyer E, Schlichthorl G, Gao Y, Karschin A, Jacob R, Schwappach B, Daut J, Preisig-Muller R. 2006. The retention factor p11 confers an endoplasmic reticulum-localization signal to the potassium channel TASK-1. Traffic 7:168–181.

Russo SJ, Nestler EJ. 2013. The brain reward circuitry in mood disorders. Nat Rev Neurosci 14:609–625.

Sarter M. 2008. The substantia innominata remains incognita: pressing research themes on basal forebrain neuroanatomy. Brain Struct Funct 213:11–15.

Schmidt EF, Warner-Schmidt JL, Otopalik BG, Pickett SB, Greengard P, Heintz N. 2012. Identification of the cortical neurons that mediate antidepressant responses. Cell 149:1152–1163.

Senn V, Wolff SB, Herry C, Grenier F, Ehrlich I, Grundemann J, Fadok JP, Muller C, Letzkus JJ, Luthi A. 2014. Long-range connectivity defines behavioral specificity of amygdala neurons. Neuron 81:428–437.

Surette AP, Madureira PA, Phipps KD, Miller VA, Svenningsson P, Waisman DM. 2011. Regulation of fibrinolysis by S100A10 in vivo. Blood 118:3172–3181.

Svenningsson P, Chergui K, Rachleff I, Flajolet M, Zhang X, El Yacoubi M, Vaugeois JM, Nomikos GG, Greengard P. 2006. Alterations in 5-HT1B receptor function by p11 in depression-like states. Science 311:77–80.

Svenningsson P, Kim Y, Warner-Schmidt J, Oh YS, Greengard P. 2013. p11 and its role in depression and therapeutic responses to antidepressants. Nat Rev Neurosci 14:673–680.

Svenningsson P, Berg L, Matthews D, Ionescu DF, Richards EM, Niciu MJ, Malinger A, Toups M, Manji H, Trivedi MH, Zarate CA Jr, Greengard P. 2014. Preliminary evidence that early reduction in p11 levels in natural killer cells and monocytes predicts the likelihood of antidepressant response to chronic citalopram. Mol Psychiatry 19:962–964.

Tye KM, Deisseroth K. 2012. Optogenetic investigation of neural circuits underlying brain disease in animal models. Nat Rev Neurosci 13:251–266.

Tye KM, Prakash R, Kim SY, Fenno LE, Grosenick L, Zarabi H, Thompson KR, Gradinaru V, Ramakrishnan C, Deisseroth K. 2011. Amygdala circuitry mediating reversible and bidirectional control of anxiety. Nature 471:358–362.

Tyzack GE, Sitnikov S, Barson D, Adams-Carr KL, Lau NK, Kwok JC, Zhao C, Franklin RJ, Karadottir RT, Fawcett JW, Lakatos A. 2014. Astrocyte response to motor neuron injury promotes structural synaptic plasticity via STAT3-regulated TSP-1 expression. Nat Commun 5:4294.

Virk MS, Sagi Y, Medrihan L, Leung J, Kaplitt MG, Greengard P. 2016. Opposing roles for serotonin in cholinergic neurons of the ventral and dorsal striatum. Proc Natl Acad Sci U S A 113:734–739.

Warner-Schmidt JL, Flajolet M, Maller A, Chen EY, Qi H, Svenningsson P, Greengard P. 2009. Role of p11 in cellular and behavioral effects of 5-HT4 receptor stimulation. J Neurosci 29:1937–1946.

Warner-Schmidt JL, Schmidt EF, Marshall JJ, Rubin AJ, Arango-Lievano M, Kaplitt MG, Ibanez-Tallon I, Heintz N, Greengard P. 2012. Cholinergic interneurons in the nucleus accumbens regulate depression-like behavior. Proc Natl Acad Sci U S A 109:11360–11365.

Warner-Schmidt JL, Vanover KE, Chen EY, Marshall JJ, Greengard P. 2011. Antidepressant effects of selective serotonin reuptake inhibitors (SSRIs) are attenuated by antiinflammatory drugs in mice and humans. Proc Natl Acad Sci U S A 108:9262–9267.

Werner HB, Kuhlmann K, Shen S, Uecker M, Schardt A, Dimova K, Orfaniotou F, Dhaunchak A, Brinkmann BG, Mobius W, Guarente L, Casaccia-Bonnefil P, Jahn O, Nave KA. 2007. Proteolipid protein is required for transport of sirtuin 2 into CNS myelin. J Neurosci 27:7717–7730.

Zamanian JL, Xu L, Foo LC, Nouri N, Zhou L, Giffard RG, Barres BA. 2012. Genomic analysis of reactive astrogliosis. J Neurosci 32:6391–6410.

Zhang L, Li H, Su TP, Barker JL, Maric D, Fullerton CS, Webster MJ, Hough CJ, Li XX, Traumatic Stress Brain Study G, Ursano R. 2008. p11 is up-regulated in the forebrain of stressed rats by glucocorticoid acting via two specific glucocorticoid response elements in the p11 promoter. Neuroscience 153:1126–1134.

Zhang L, Li CT, Su TP, Hu XZ, Lanius RA, Webster MJ, Chung MY, Chen YS, Bai YM, Barker JL, Barrett JE, Li XX, Li H, Benedek DM, Ursano R. 2011a. P11 expression and PET in bipolar disorders. J Psychiatr Res 45:1426–1431.

Zhang L, Su TP, Choi K, Maree W, Li CT, Chung MY, Chen YS, Bai YM, Chou YH, Barker JL, Barrett JE, Li XX, Li H, Benedek DM, Ursano R. 2011b. P11 (S100A10) as a potential biomarker of psychiatric patients at risk of suicide. J Psychiatr Res 45:435–441.

Zhang Y, Chen K, Sloan SA, Bennett ML, Scholze AR, O'Keeffe S, Phatnani HP, Guarnieri P, Caneda C, Ruderisch N, Deng S, Liddelow SA, Zhang C, Daneman R, Maniatis T, Barres BA, Wu JQ. 2014. An RNA-sequencing transcriptome and splicing database of glia, neurons, and vascular cells of the cerebral cortex. J Neurosci 34:11929–11947.

Zimmer DB, Chaplin J, Baldwin A, Rast M. 2005. S100-mediated signal transduction in the nervous system and neurological diseases. Cell Mol Biol 51:201–214.

Zobiack N, Rescher U, Ludwig C, Zeuschner D, Gerke V. 2003. The annexin 2/S100A10 complex controls the distribution of transferrin receptor-containing recycling endosomes. Mol Biol Cell 14:4896–4908.

Zonouzi M, Scafidi J, Li P, McEllin B, Edwards J, Dupree JL, Harvey L, Sun D, Hubner CA, Cull-Candy SG, Farrant M, Gallo V. 2015. GABAergic regulation of cerebellar NG2 cell development is altered in perinatal white matter injury. Nat Neurosci 18:674–682.